Statistical Model of Land Surface Temperature in Sumatra Island, Indonesia: 2000-2018

Tofan Agung Eka Prasetya

A Thesis Submitted in Fulfillment of the Requirements for the
Degree of Doctor of Philosophy in Research Methodology
Prince of Songkla University
2021

Thesis Title   Statistical Model of Land Surface Temperature in Sumatra Island, Indonesia: 2000-2018

Author   Mr. Tofan Agung Eka Prasetya

Major Program   Research Methodology

Major Advisor:

…...……………………….
(Asst. Prof. Dr. Sarawuth Chesoh)

Co-advisors:

…...……………………….
(Assoc. Prof. Dr. Apiradee Lim)

…...……………………….
(Emiritus Prof. Dr. Don McNeil)

Examining Committee:

…...…………………….Chairperson
(Prof. Dr. Ririh Yudhastuti)

…...…………………….
(Asst. Prof. Dr. Sarawuth Chesoh)

…...…………………….
(Assoc. Prof. Dr. Apiradee Lim)

…...…………………….
(Emiritus Prof. Dr. Don McNeil)

…...…………………….
(Asst. Prof. Dr. Mayuening Eso)

The Graduate School, Prince of Songkla University, has approved this thesis as fulfillment of the requirements for the Doctor of Philosophy Degree in Research Methodology

……………..…………………………...
(Prof. Dr. Damrongsak Faroongsarng)
Dean of Graduate School

This is to certify that the work here submitted is the result of the candidate's own investigations. Due acknowledgement has been made of any assistance received.

…………...………………………..
(Assist. Prof. Dr. Sarawuth Chesoh)
Major Advisor

…………...………………………..
(Mr. Tofan Agung Eka Prasetya)
Candidate

I hereby certify that this work has not been accepted in substance for any other degree and is not being currently submitted in candidature for any degree.

…………………….............

(Mr. Tofan Agung Eka Prasetya)

Candidate

Thesis Title   Statistical Model of Land Surface Temperature in Sumatra

         Island, Indonesia: 2000-2018

Author   Mr. Tofan Agung Eka Prasetya

Major Program Research Methodology

Academic Year 2021

ABSTRACT

Global warming could be assessed by estimating the Land Surface Temperature (LST) change in a regional and global area. The aims of this study were (1) to determine seasonal patterns and trends in time-series data LST in Sumatra Island and (2) in Sumatra Island, Indonesia, to study the relationships between LST, elevation, land cover (LC), and the Normalized Difference Vegetation Index (NDVI). The data were obtained from NASA Moderate Resolution Imaging Spectroradiometer (MODIS) website and focused on during 2000-2018.

The cubic splines had been applied to investigate the seasonal patterns and time series trends of LST change and simple linear regression had been applied to analyze the relationship between elevation, LC, and NDVI with LST change in Sumatra Island. In 2018, approximately 44.6% of Sumatera area was evergreen broadleaf forest where the urban area only covered 0.51% of the whole area. Cubic spline result identifying the trend indicated that 36.2% of Sumatera experiencing decreasing of LST change and other 27.7% increasing of LST change. Furthermore, linear regression identified the factors which concluded the lowest LST change occurred in elevation 60-109 meter above sea level (MASL) evergreen broadleaf forest with NDVI less than 0.75 and the highest change occurred in 320+ MASL Savannas with NDVI 0.8-1.0. Based on the 3 determinants, LST decreased by 0.122 °C on an overall mean per decade.

The findings can be applied to monitor environmental changes, particularly the state of the regional climate change relating to planting crops, agricultural expansion and deforestation. However, the other factors need to be taken into account in the model.

Acknowledgements

Bismillahirrahmanirrahiim, in the name of Alloh, the most gracious, the most merciful. Sholawat and Salam send to His big messenger Prophet Muhammad SAW for being the human's idol in a lifetime. Alhamdulillah, all praises belong to Alloh. I really feel grateful to Alloh for blessing me with a chance, time, health, knowledge and facing many kinds of people. The thesis would not be complete without the assistance and guidance from several people. In this marveleous opportunity, I wish to acknowledge them.

First, I would like to express my gratitude to my astonishing advisor and co-advisors, Assist. Prof. Dr. Sarawuth Chesoh, Assoc. Prof. Dr. Apiradee Lim, and Prof. Dr. Don McNeil for their entire inception ideas. They consistently steered me in the right direction whenever he thought I needed it. I would also love to extend my gratitude to Assist. Prof. Dr. Phattrawan Tongkumchum, Dr. Attachai Ueranantasun, Assist. Prof. Dr. Rhysa McNeil and all lectures or academic staff in the Department of Mathematics and Computer Science for being such lovely teachers and family.

Second, my deep gratitude expressed to Prince of Songkla University for supporting the study with TEH-AC Scholarship for international students and Graduate School, Prince of Songkla University for providing research funding.

Thirdly, the biggest thanks go to my beloved wife and my son who is never tired for giving support, encouragement, unconditional love and faithful prayers for me. Thanks also to our parents and all brothers and sisters for never ending prayers for me.

Finally, I would like to give a parcel of thanks to people who always help us in three years, they are Indonesian Student Association PSU (Permitha) and all friends in both the Research Methodology and Applied Mathematics programs.

Tofan Agung Eka Prasetya

Table of Contents

List of Tables

List of Figures

Chapter 1

Introduction

1.1 Research background

One of the urgent environmental problems facing the globe is climate change, particularly rising air temperature. At regional to global scales, air temperature, particularly Land Surface Temperature (LST), is crucial for assessment of climatological processes, land surface energy exchanges, and water stability in relation to climate change implications (Gao et al., 2008; Li et al., 2013; Wongsai et al., 2017). The global warming and climate change also affect human lives and have a large impact on society as a whole (Marjuki et al., 2016). The slowdown of long-term declines in the incidence of undernutrition, which is partially linked to harsh weather, reflects this (Wheeler & Braun, 2013). Regarding this issue, Southeast Asia as a global exporter has a critical role to maintain the vulnerable sector agriculture and food security.

Some possible determinants for analyzing LST include Normalized Difference Vegetation Index (NDVI), Land Cover (LC), and elevation (Sun et al., 2012; Guan et al., 2014; Alavipanah et al., 2015). The large disparity in land elevation has a big impact on LST (Gao et al., 2008). The effects of the LC composition and configuration on LST had been investigated by several studies (Voogt and Oke, 2003; Zhou et al., 2011; Sobrino set al., 2013). The effect directions of LC on estimating LST were proposed to be consistent across seasons, but the magnitude of effects differed by season, delivering the highest level of predictability during summer and the weakest during winter (Zhou et al., 2014).

Several research have been conducted to illustrate how NDVI affects surface temperature and how extreme temperatures affect land surfaces (Alavipanah et al., 2015; Vasishth, 2015; Zhou et al., 2011; Zhou et al., 2014). The studies indicated that low point NDVI occurred in high-temperature areas and correspondingly high point NDVI occurred in low-temperature areas. Some research has been recommended looking at the relationship between vegetation form and LST, which has a negative impact and is linked to a variety of land uses (Weng et al., 2004; Yue et al., 2007).

Sumatra Islands has the greatest rate of deforestation in Indonesia (Rijal et al., 2016). The Islands is also the largest of three Indonesian islands that have been deforested. The conversion of Sumatra's forests to non-forest areas has piqued the interest of national and foreign researchers. A study in Sumatra investigated further into reason of rising LSTs by focusing on forest conversion, and the results indicated that forest conversion was the major reason for the particular island's LST increase (Sabajo et al., 2017).

NDVI, LC, and elevation might interact with each other. Although the previous studies had invested the effects of these factors independently. However, there have been a few studies in Indonesia on the impact of these factors. As a result, this study aimed to investigate the seasonal pattern of LST and to investigate the effect of NDVI, LC, and elevation on the changes in LST on Sumatra Island.

1.2 Research objectives

The following are the study's objectives:

1. To identify the seasonal trends of LST in Sumatra Island.
2. To investigate the relationships between LST change and environmental factors include elevation, LC and NDVI in Sumatra Island.

1.3 Expected advantages

The expected advantage of this study is to provide basic information about LST trends using cubic spline and simple linear regression models which are useful for policymakers to develop further action plans and project activities. Policymakers could apply this study results in concentrating on a particular region of Sumatra that requires to have strong environmental protection from increasing air temperature and the causes.

1.4 Scope of Study

This research used secondary MODIS data which were obtained from the NASA website where we focused on LST from 2000-2018. The data consist of LST, LC, elevation, and NDVI from Sumatera Island, Indonesia. Furthermore, the seasonal trends of LST were investigated. The relationships between LST and other variables were identified. A cubic spline function was used to examine LST time series trends.

Moreover, the simple linear regression was applied for investigating the relationship between LST change and environmental factors: elevation, LC, and NDVI in the Sumatra area.

1.5 Literature reviews

1.5.1 MODIS satellite data

MODIS data has been proposed to help us better comprehend global, tropospheric aerosols (King et al., 1999), and approaches to obtain aerosol data across land and ocean surfaces have been developed (Kaufman & Tanré, 1998). According to the MODIS-VIIRS Atmosphere Discipline Team, imager remote sensing algorithms are developed and maintained for the production of long-term climatic data records of derived geophysical parameters related to earth's atmospheric features (aerosols, clouds, water vapor). The MODIS sensor, which is housed on the Terra (and Aqua) satellite platforms, contains 36 spectral channels (compared to 4–8 for most sensors) and was created to offer a wide range of data on land, oceanic, and atmospheric variables (Engel-Cox et al., 2004; Gupta et al., 2006).

The MODIS delivers measurements with intermediate spatial (250 m-1 km) and temporal (1–2 days) resolutions in many spectral regions of the electromagnetic spectrum (Gupta et al., 2006). The MODIS instruments provide two daytime observations for a given area: 10:30 a.m. from Terra and 1:30 p.m. from Aqua (Wang and Christopher, 2003). Several studies have used MODIS satellite data to analyze air quality (Chu et al., 2003; Hutchison, 2003; Wang and Christopher, 2003; Engel-Cox et al., 2004; Gupta et al., 2006;).

1.5.2 Land Surface Temperature

The land surface temperature (LST) is measured at the interface between the atmosphere and the materials in the earth surface (top of plant canopy, water, soil, ice or snow surface) (Stroppiana et al., 2014). NASA's Earth Observation System (EOS) satellites Terra and Aqua that produced MODIS data, released in 1999 and 2002, are among the most sophisticated and extensively used LST products. There are two

product streams available for both the Level-1 and the Atmosphere Archive and Distribution System (LAADS) Distributed Active Archive Centers (DAAC). The MODIS Standard Items with EOS history and the VIIRS Continuity Products are the products in question. According to the MODIS LST product user guide, all space-borne sensors detect and assess the LST four times per day at 10:30 and 22:30 for Terra, then 13:30 and 1:30 for Aqua with local overpass-times. MODIS provides LST data time series at two spatial resolutions: 1 km and 0.05 degree latitude/longitude climate model grids/CMG) on a regular, eight-day, and monthly basis (Wan, 2008).

Previous sensors, such as the NOAA-AVHRR (National Oceanic and Atmospheric Administration-Advanced Very High-Resolution Radiometer) and SNPP-VIIRS (National Oceanic and Atmospheric Administration-Advanced Very High-Resolution Radiometer) and SNPP-VIIRS (National Oceanic and Atmospheric Administration-Advanced Very High-Resolution Radiometer) and SNPP-VIIRS (The Suomi National Polar-orbiting Partnership-Visible Infrared Imaging Radiometer Suite). Furthermore, climate data is frequently processed to produce a set of standard products for monitoring land, atmosphere, and oceans (Justice et al., 2002).

On regional and global dimensions, LST is a crucial parameter in the physics of land surface processes (Wan et al., 2004). LST refers to the radiation radiated by the land surface as seen by MODIS at different viewing angles. The land surface in vegetated areas refers to the canopy, whereas the land surface in bare areas refers to the soil surface. This model incorporates all surface–atmosphere interactions as well as energy flows between the atmosphere and the ground. The LST calculated from satellite data can be used to confirm and improve global weather forecasts. The LST acquired from satellite data can be used to test and improve the global meteorological model prediction after suitable aggregation and parameterization.

1.5.3   *Normalized Difference Vegetation Index*

Vegetation, which is a wide term for plant ground cover, is the earth's most abundant biotic element. Vegetation is involved in most of the processes that drive climate change, including temperature fluctuations. The NDVI is a technique for analyzing and

forecasting current and historical vegetation conditions. The NDVI is determined with MODIS sensors, which capture the spectral behavior of vegetation. In theory, plants react differently to different sections of the electromagnetic spectrum, according to the evidence provided (including visible light). Because the red and blue wavelengths of electromagnetic waves are frequently absorbed, reflected light preserves the green wavelengths, with significant reflection in the near infrared (NIR) wavelengths.

Understanding the state of the vegetation in a given area necessitates satellite or remote sensing mapping and monitoring. The inventory of green cover, production forecasts, and vegetation growth evaluation are all examples of satellite imaging results from vegetation monitoring (Ozyavuz et al., 2015). The index values vary from -1 to 1, however for vegetation, the range is usually 0.1 to 0.7. Values near 0 suggest an area that reflects both near-infrared and red levels, but high index values indicate good vegetation cover (bare soil and rock). Negative numbers represent the polar opposite of vegetation (clouds, water, and snow) (Adeyeri and Okogbue, 2014).

1.5.4   Land Cover

Changes in land cover are one of the most serious and urgent dangers to the natural environment, as well as the ecosystem services that humans rely on (Newbold et al., 2016; Pribulick et al., 2016). Remote sensing-based land cover studies have a long history and have made significant progress (Sun et al., 2016). Land-use and land-cover change (LUCC) is a key measure of how humans interact with the environment (Dewan et al., 2012).

The amount of forest, wetlands, impermeable surfaces, agricultural and other land, and water types that cover a region is shown by land cover data. Different types of water include wetlands and open water. The way humans use the land for development, conservation, or a combination of the two is referred to as land use. Various types of land cover can be preserved and utilized in a variety of ways.

Satellite and aerial photography, according to the National Oceanic and Atmospheric Administration (NOAA), could be used to determine land cover. Land usage cannot be assessed using satellite photos. Managers can utilize land cover maps to gain a better

understanding of the current landscape. To show changes over time, land cover maps spanning several years are required (National Oceanic and Atmospheric Administration National Centers for Environmental Information (NOAA NCEI), 2020).

1.5.5   Elevation

The vertical distance between a place on the ground surface and a reference point, usually the mean sea level, is known as elevation (or altitude) (Mcvicar & Jupp, 1998). Digital Elevation Models are satellite-based elevation data produced by the USGS earth explorer (DEM). The final outcome is a numerical representation of a surface laid out in a series of regular grids, each containing a three-dimensional object. DEMs are critical topographic inputs for accurate floodplain hydrodynamic modeling, where they play a key role as natural retarding pools that attenuate flood waves and decrease flood peaks (Demir & Akyurek, 2016).

1.5.6   Factors related to LST

The land surface temperature is influenced by the energy balance of the earth's surface, surface thermal characteristics, and atmospheric conditions (Srivastava et al., 2009). Since the pre-industrial era, global and local changes in the earth's climate have continued. Natural and manmade factors such as greenhouse gases, land cover and land use change, unregulated groundwater usage, deforestation, increased water demand, urbanization, and irrigation operations all contribute to changes (Hansen et al., 2013; Lambin et al., 2003; Näschen et al., 2019).

In the study of thermal and environmental behavior, LST is a significant parameter. The effects of increasing and decreasing LST in the lower atmosphere on surface radiation, energy exchange, climate, and human comfort are all significant factors to consider (Voogt and Oke, 2003). LSTs are influenced by a number of elements, including the physical features of various types of urban surfaces, their color, the sky view factor, street geometry, traffic loads, and anthropogenic activities (Chudnovsky et al., 2004). The distribution of LULC characteristics closely reflects the LST of urban surfaces (land use and land cover) (Lo et al., 1997; Q Weng, 2001; Yunhao et al., 2007).

Biophysical and climatological parameters such as urban and street geometry (Eliasson, 1996), built-up area and height (Bottyán & Unger, 2003), LULC (Dousset & Gourmelon, 2003), and vegetation (Bottyán & Unger, 2003; Weng et al., 2004). More studies are required to determine LST's relationship with other biophysical and/or socioeconomic variables utilizing an integrated remote sensing technology in order to gain a better understanding of its impact.

1.5.7   Statistical modelling in LST

Statistical approaches that take into account the geographical and time frame that has been derived often perform well (Stisen et al., 2007). Zhang et al. (2016) undertook a study to increase the accuracy of calculating daily air temperatures over the Tibetan Plateau. The Tibetan Plateau resembles Sumatra Island in terms of climate. They used the simple linear regression model since it is straightforward to comprehend and is the most prevalent strategy used in previous investigations. They argued that linear regression was only accurate when night data from the LST was given. Using MODIS LST, Fu et al. (2011) used linear regression to predict air temperature in an alpine meadow on the Northern Tibetan Plateau. They did, however, claim that the MODIS LST data is incorrect. As a result, they advised that the peak air temperature be taken into account.

Cubic spline is another statistical model that can be used to study the seasonal pattern of climate-related satellite data (Wongsai et al., 2017; Sharma et al., 2018). Sharma et al. (2018) cubic spline can be utilized to detect seasonal patterns of LST variation. Curvilinear trend was replaced by cubic spline, which was less biased and more efficient (Howe et al., 2011). Suwanwong and Kongchouy (2016) investigated LST pattern and variation using a combination of cubic spline and generalized estimated equation (GEE) because cubic spline regression allows for a good perception of temperature pattern and variation.

Users can define derivatives for a k-th order spline model, which is a famous arithmetic curve fitting with derivatives function (Wahba, 1990). The user can customize not only the spline function's degree, but also the amount of polynomial pieces joining points

(known as knots), the places of the knots, and the spline function's free coefficients (Wold, 1974). A cubic spline of order 3 is the most widely used spline. The smoothest integrated squared second derivative of all functions is a cubic spline function, which is a piecewise cubic polynomial with continuous second derivatives. Using linear least squares regression, it's also simple to fit (Smith Jr. et al., 1974). The cubic spline function is extensively used for smoothing data in disciplines such as interactive computer graphics (Smith Jr. et al., 1974), real-time digital signal processing, and satellite-based time series data. The spline fit's main advantages are its continuous first and second derivatives, as well as its ease of calculation, excellent stability, high precision, and smoothness. In contrast to the sharply coupled straight line segments seen in parabolic spline smoothing, the gradients derived from cubic spline functions are smooth linked parabolas. To fit a smooth spline curve in the plot, the number of knots and their locations are selected through trial and error.

This chapter discusses the study's background and justification, as well as the study's objectives, predicted benefits, scope, and literature reviews. The data source, data administration, variables, and statistical methods will all be covered in the following chapter. In Chapter 2, you'll learn about cubic spline and simple linear regression. The findings of this investigation are described in Chapter 3. The final chapter, Chapter 4, will discuss and complete the entire study.

Chapter 2
Methodology

2.1 Data Sources

The study used satellite-based data which was retrieved from MODIS. LST daytime data was employed on this research, because the land surface absorbs solar radiation during the day and releases it through long-wave radiation at night (Huang et al., 2015). LST and LC were retrieved from ORNL DAAC with MOD11A2 code, and NDVI data were retrieved from MOD13Q1. Lastly, elevation data were obtained from US the Geological Survey (USGS) earth explorer website (Wan, 2008; ORNL DAAC, 2018; Phan et al., 2018). The covered area extended 52 km from the center in all four directions (east, west, north, and south).

LST data were collected from 8-day Tera LST (MOD11A2) from 2000 to 2018 at $0.05°$ spatial resolution. LC consists of 17 groups including uncategorized areas and elevation value starting from zero. Elevation was converted from image to values of Meter above Sea Level (MASL) which represent the height of the area. These three variable LST, LC, and elevation had 1000 m resolution per pixel and NDVI had 250 m resolution per pixel.

Regarding huge data size, the NDVI data (MOD13Q1) were treated differently where one area (called super-region) was divided into 4 areas (namely a, b, c, and d). Latitude and longitude of LST data were used as reference to estimate four points of NDVI latitudes and longitudes.

These are several terms used in this research.
a. *Super region* is an area covering 105 km $\times$ 105 km using a specific coordinate, latitude and longitude as a central point. Sumatera Island consists of 70 super region and each of them covers 25 regions.
b. *Region* is an area with a large 21 km $\times$ 21 km and this area comprises 9 sub-regions.
c. *Sub-region* is an area with dimension 7 km x 7 km which contains 49 pixels with area 1 km $\times$ 1 km.

d.   *Pixel* is our research unit which is compressed all satellite data (LST, elevation, LC, and NDVI) in time series record from 2000-2018.

The data were retrieved one-by-one for each super region (70 super regions in this study). The data mining process was depicted in Figure 2.1.
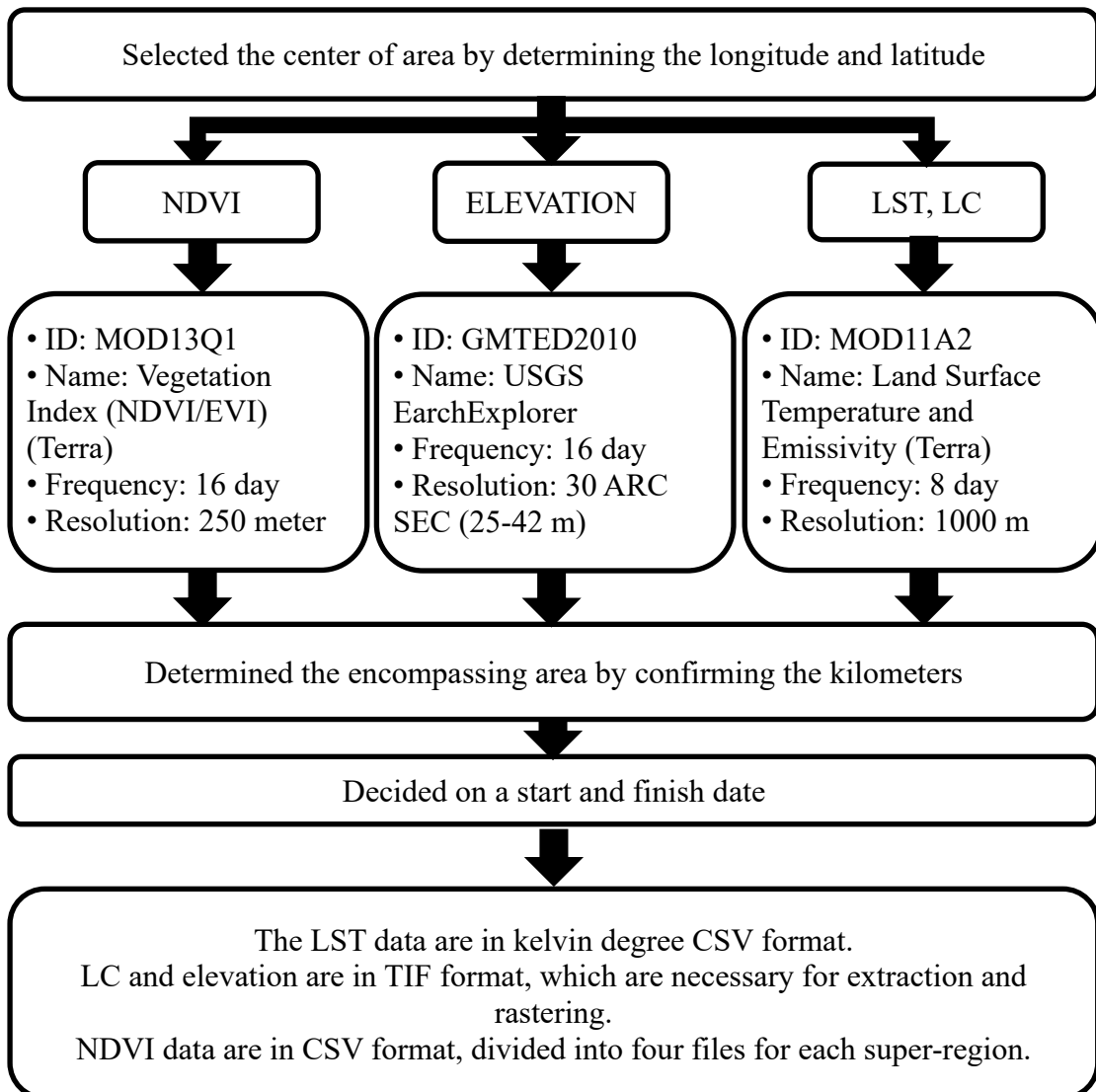
Figure 2.1 Steps of data mining and analysis for LST, elevation, LC, and NDVI in 2000-2018.

2.2 Data management

LST data are from 8-day Tera LST (MOD11A2) from 2000 to 2018 at 0.05° spatial resolution. LST degrees were originally measured in Kelvin and subsequently converted to Celsius. MODIS 8-day LST data are a mean of the clear-sky condition

data only. Elevation data were extracted from LST data. Figure 2.2 showed the way to manage data for analysis.

Figure 2.2 Flow chart of data management

The data management for each variable is shown in the following figures.

```
┌─────────────────┐           ┌─────────────────────┐
│  LST raw data   │-----------│ Raw data in total   │
│    MOD11A2      │           │    59469 records    │
└─────────────────┘           └─────────────────────┘
         │
         ▼
┌─────────────────┐           ┌─ ─ ─ ─ ─ ─ ─ ─ ─ ─ ─┐
│  Cubic Spline   │           │ Adjusted each        │
│ for analysis    │-----------│ observation with     │
│ seasonal trend  │           │ Pixels, determined   │
│                 │           │ suitable knots, and  │
└─────────────────┘           │ adjusted LST change  │
         │                    └─ ─ ─ ─ ─ ─ ─ ─ ─ ─ ─┘
         ▼
┌─────────────────┐           ┌─ ─ ─ ─ ─ ─ ─ ─ ─ ─ ─┐
│   LST change    │           │ Classify into three  │
│   categories    │-----------│ group, increase,     │
│                 │           │ stable and decrease  │
│                 │           │ to identify seasonal │
└─────────────────┘           │      trend           │
         │                    └─ ─ ─ ─ ─ ─ ─ ─ ─ ─ ─┘
         ▼
┌─────────────────┐           ┌─ ─ ─ ─ ─ ─ ─ ─ ─ ─ ─┐
│ Compile with    │           │ Adjusted-daily-LST   │
│ the predictor   │-----------│ change compile with  │
│                 │           │ LC, Elevation, and   │
│                 │           │      NDVI            │
└─────────────────┘           └─ ─ ─ ─ ─ ─ ─ ─ ─ ─ ─┘
         │
         ▼
┌─────────────────┐
│                 │
│   Modelling     │
│                 │
└─────────────────┘
```
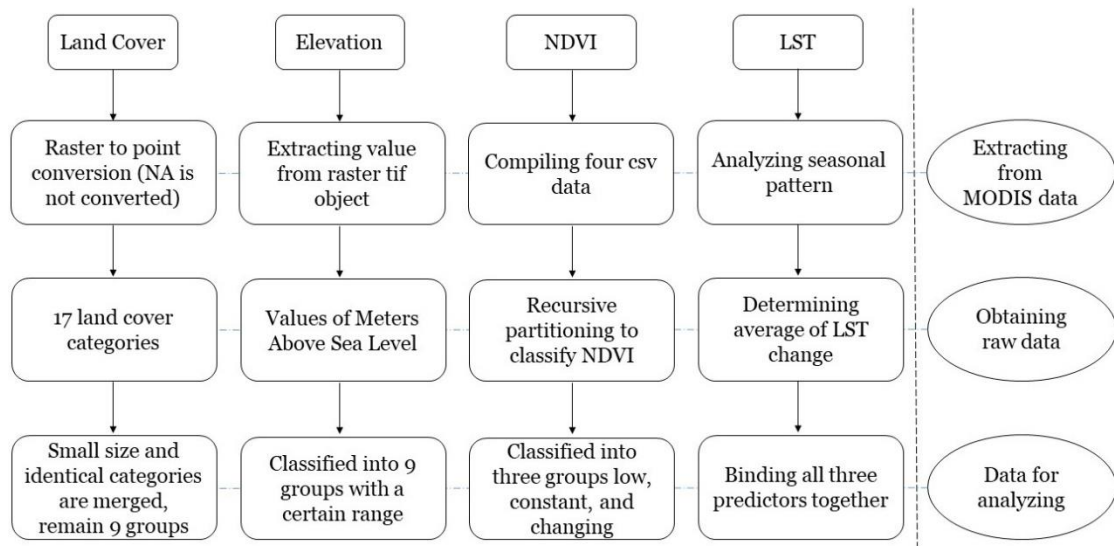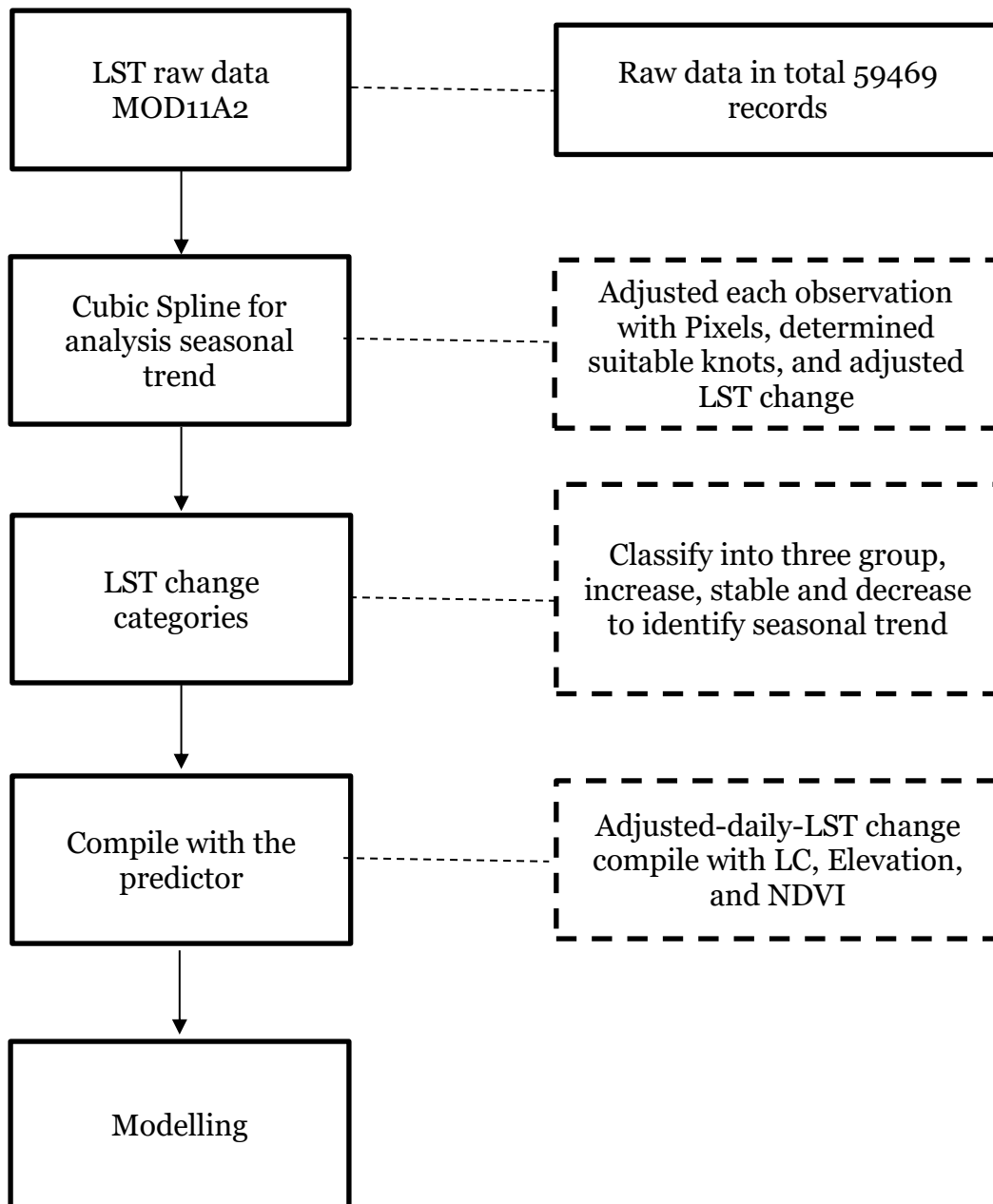
Figure 2.3 Process of managing LST data and analysis

Firstly, LST data was adjusted to the Pixel coordinate latitude longitude. Cubic spline determined the LST change which will be used as an output variable in a simple linear regression.
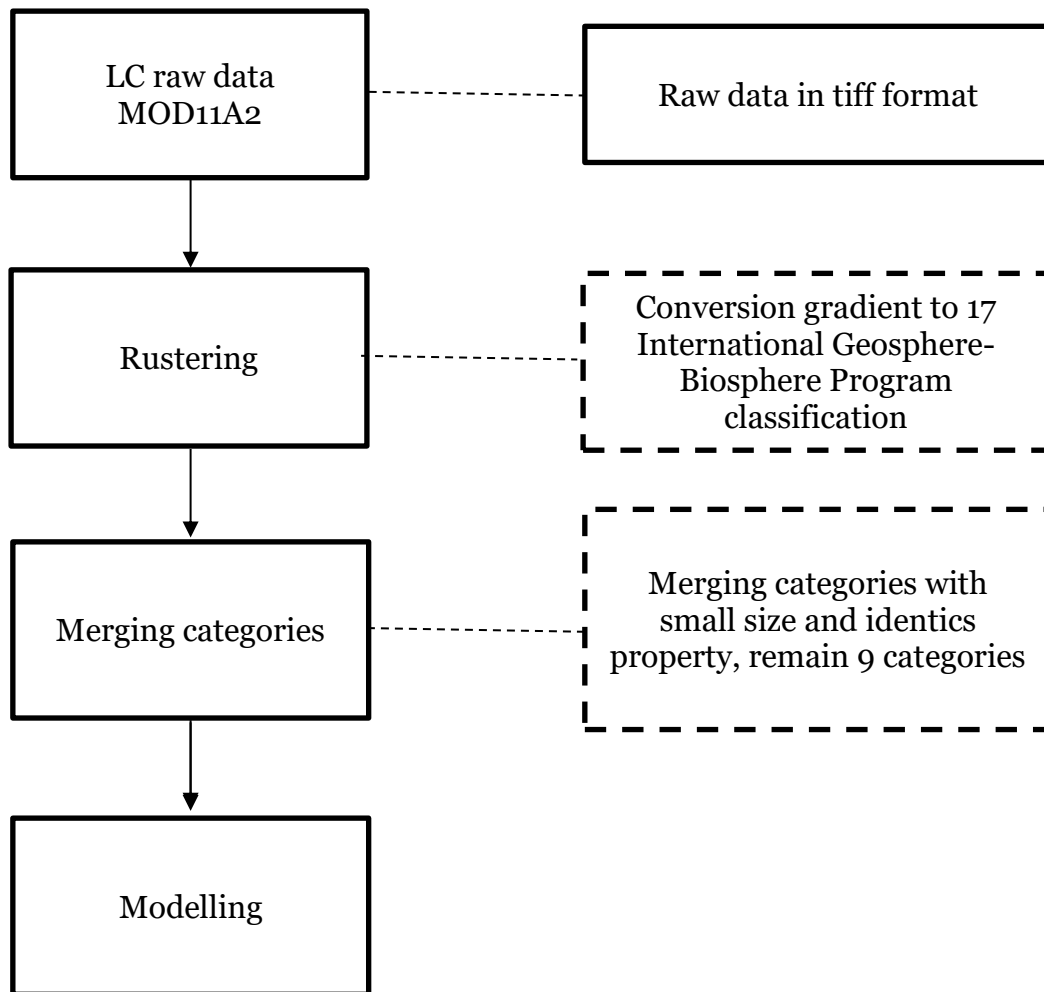
Figure 2.4 Process of managing LC data and analysis

MODIS LC dataset can be ordered as a set of MOD11A2. The seventeen LC types are based on International Geosphere-Biosphere Program classification: evergreen needleleaf forest (EN. Forest), evergreen broadleaf forest (EB. Forest), deciduous needleleaf forest (DN. Forest), deciduous broadleaf forest (DB. Forest), mixed forest, closed shrublands (C. Shriblands), open shrublands, woody savannas (W. Savannas), savannas, grasslands, permanents wetlands (P.Wetlands), croplands, urban and built-up, cropland or natural vegetation mosaic (Crop Mos), snow and ice, barren or sparsely vegetated and water bodies (Friedl et al., 2005; Y. Li et al., 2016).

Moreover, due to Sumatera Island characteristics, several LC categories were merged despite its small size and identics property. Evergreen Needleleaf Forest, Evergreen Broadleaf Forest, Deciduous Needleleaf Forest, Deciduous Broadleaf Forest, Mixed

Forest, and Closed Shrubland were merged into one group as Evergreen Broadleaf Forest. Barren or sparsely vegetated was combined with Grasslands. Then, other categories remain the same. The open Shrubland and Snow and Ice categories do not exist on Sumatera Island. Furthermore, LC with 9 categories was used to predict the LST change using simple linear regression.

```
┌─────────────────────┐           ┌─────────────────────────┐
│  Elevation raw data │- - - - - -│   Raw data in Tiff format│
│     GMTED2010       │           │                         │
└─────────────────────┘           └─────────────────────────┘
           │
           ▼
┌─────────────────────┐           ┌ ─ ─ ─ ─ ─ ─ ─ ─ ─ ─ ─ ─ ┐
│                     │             Conversion gradient to
│      Rastering      │- - - - - - number of MASL, tiff format
│                     │             to csv format
└─────────────────────┘           └ ─ ─ ─ ─ ─ ─ ─ ─ ─ ─ ─ ─ ┘
           │
           ▼
┌─────────────────────┐           ┌ ─ ─ ─ ─ ─ ─ ─ ─ ─ ─ ─ ─ ┐
│  Value of Meter Above│            Each Super region has 11,025
│     Sea Level       │- - - - - - records with total 771,750
│                     │             records
└─────────────────────┘           └ ─ ─ ─ ─ ─ ─ ─ ─ ─ ─ ─ ─ ┘
           │
           ▼
┌─────────────────────┐           ┌ ─ ─ ─ ─ ─ ─ ─ ─ ─ ─ ─ ─ ┐
│                     │             Classified into 9 groups with
│ Group classifications│- - - - - - a certain range, small
│                     │             number of observations are
└─────────────────────┘             merged
           │                       └ ─ ─ ─ ─ ─ ─ ─ ─ ─ ─ ─ ─ ┘
           ▼
┌─────────────────────┐
│                     │
│     Modelling       │
│                     │
└─────────────────────┘
```
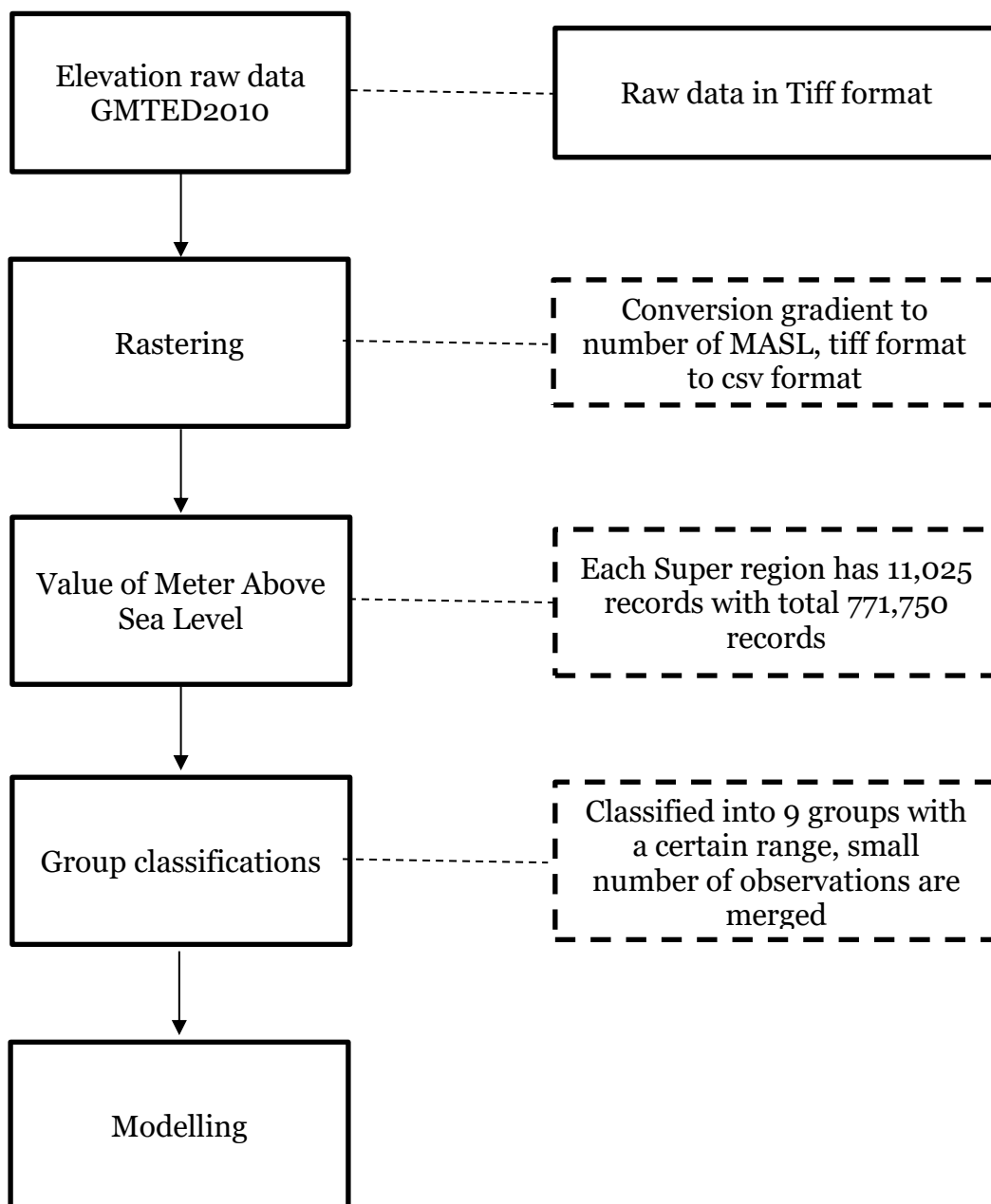
Figure 2.5 Process of managing elevation data and analysis

Elevation was converted from the image to values of MASL which represent the height of the area. For descriptive analysis, MASL values were classified into seven groups regarding its color gradation where 1. <15 MASL; 2. 15-39 MASL; 3. 40-89 MASL; 4. 90-179 MASL; 5. 180-349 MASL; 6. 350-649 MASL; 7. >650 MASL. Furthermore, elevation was categorized into nine groups in MASL: 1. <15 MASL; 2. 15-19 MASL; 3. 20-34 MASL; 4. 35-59 MASL; 5. 60-109 MASL; 6. 110-319 MASL; 7. 320-739 MASL; 8. 740-1119 MASL; 9. 1120+ MASL for analysis purpose.
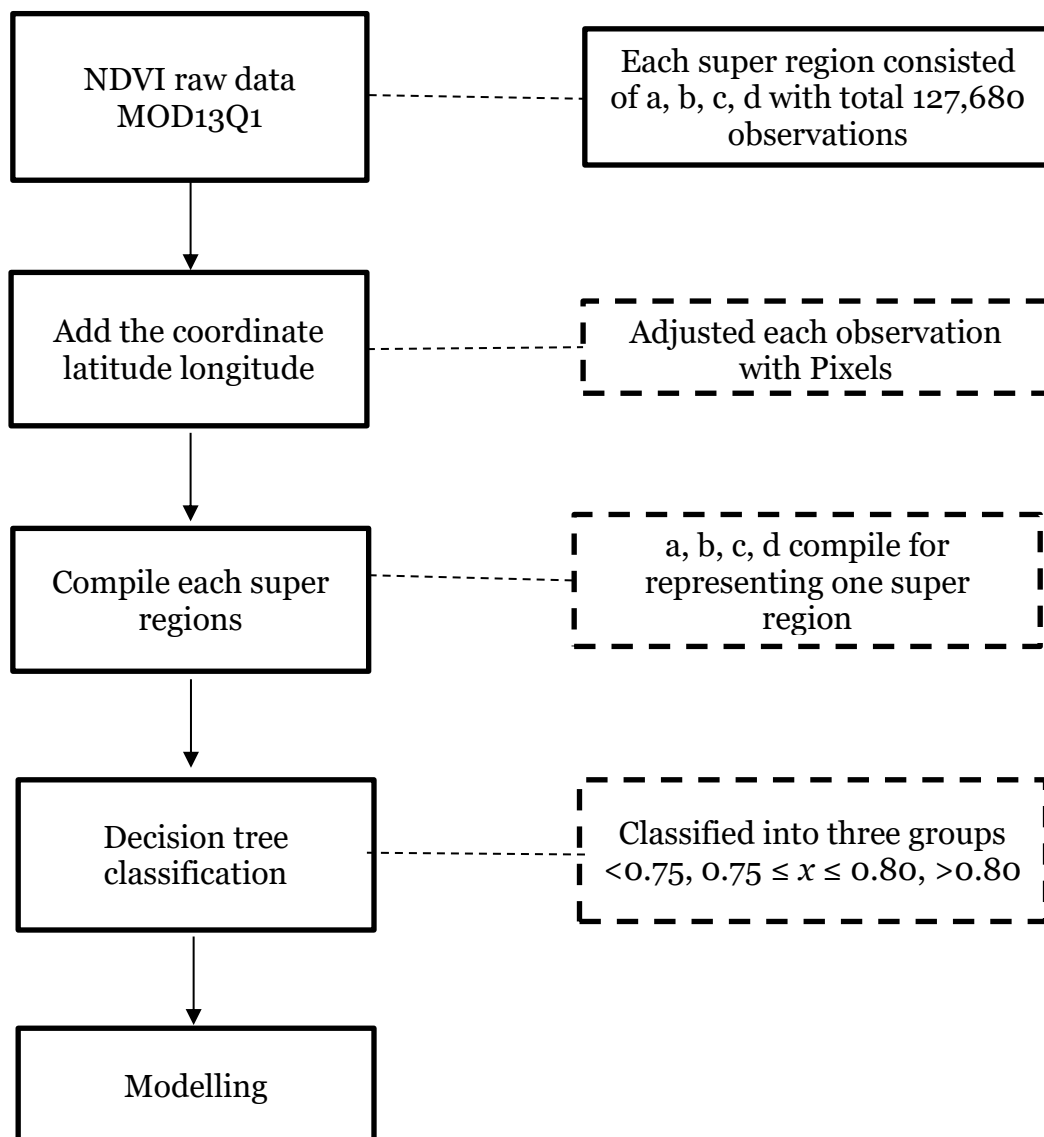
Figure 2.6 Process of managing NDVI data and analysis

MODIS NDVI dataset (MOD13Q1) was ordered separately from LST and LC at a spatial resolution of 0.05°. Each variable was bound by pixel which modified according to large area of 1 km square to produce adjusted values for each variable in each pixel. The NDVI was categorized into less than 0.75, 0.75-0.80, and more than 0.80. The index values ranged from -1 to 1, but for vegetation, the index ranges from 0.1 to 0.7. High index values are covered by healthy vegetation. Around infrared and red levels are both reflected in an area with values near zero (bare soil and rock). Negative values are for the other which is the contrary of vegetation (clouds, water, and snow) (Adeyeri and Okogbue, 2014).

2.3 Study area

The MODIS data used in this study focused on Sumatra Island. The Sumatra archipelago consists of Sumatra's islands as well as nearby tiny islands. As indicated in Figure 2.3, Sumatra Island is located between east longitude 950 and 109.20 east longitude and north latitude 60 and 6.20 south latitude. The islands of Sumatra are divided into ten provinces and 152 regencies/cities. The Sumatra Islands are 47,693,691.34 hectares wide.
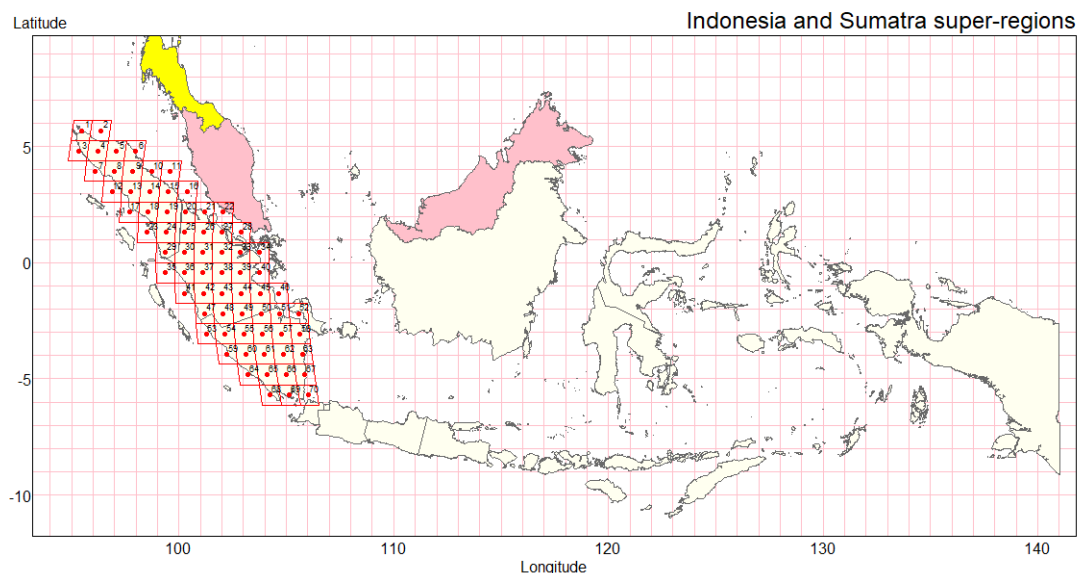

Figure 2.7 Study area of Indonesia and Sumatra super regions.

Figure 2.7 depicts Sumatra as an extended continent covering a diagonal northwest-southeast axis. The Indian Ocean runs along Sumatra's west, northwest, and southwest

shores, with the Simeulue, Nias, and Mentawai Island group off the western coast. The Malay Peninsula is a peninsula that extends from the Eurasian continent, separated from the island in the Northeast by the narrow Strait of Malacca. Sumatra and Java are separated in the southeast by the short Sunda Strait. To the north of Sumatra are the Andaman Islands, while to the south are the islands of Bangka and Belitung, the Karimata Strait, and the Java Sea. The Bukit Barisan Mountains, which have multiple active volcanoes, form the Bukit Barisan Mountains, while the northeastern part contains vast plains and lowlands with swamps, mangrove forests, and complex river systems. In the provinces of West Sumatra and Riau, the equator runs through the island's center. The island's climate is tropical, hot, and humid. Once upon a time, the landscape was dominated by lush tropical rain forests.
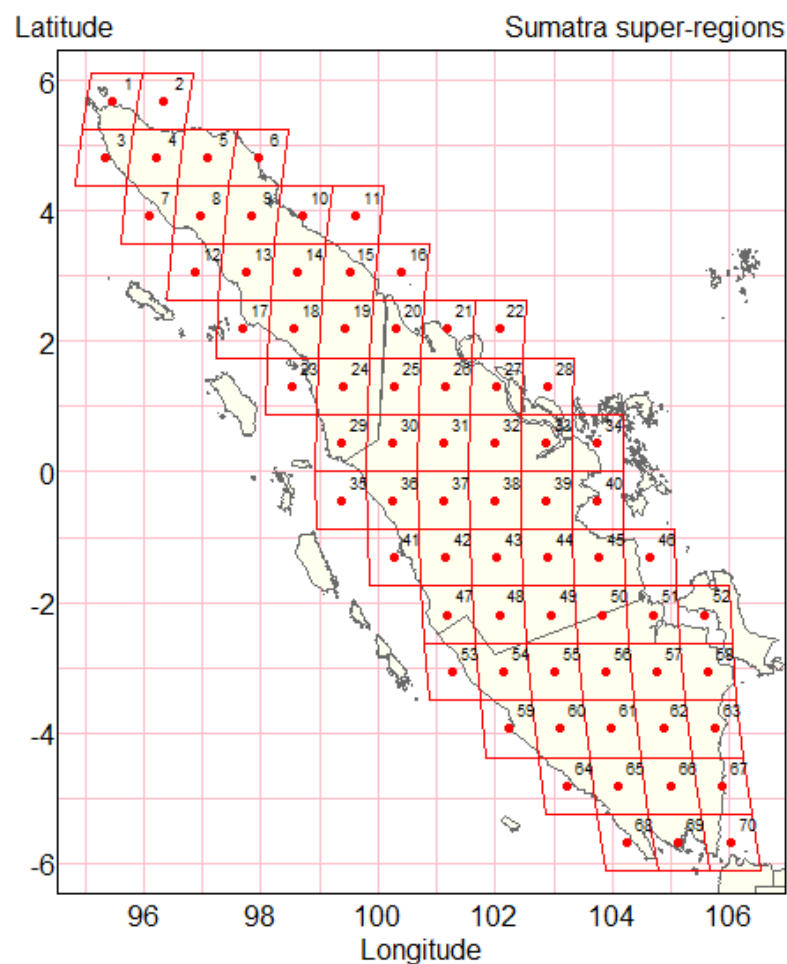

Figure 2.8 Super regions of Sumatra with the center of latitude and longitude.

2.4 Variables

Variables used in this study are Time, Elevation, NDVI, LC and LST where each region has different number of observations. There are two main objectives, identifying the trend of LST and identifying factors (LC, elevation, NDVI) related to LCT change. Path diagrams in this study as shown in Figure 2.9 and Figure 2.10 depict the outcome and determinants. The determinant of the first object is time and the outcome is LST where a cubic spline was applied to analyze the seasonal trends. LST changes were obtained from cubic spline model and were used as an outcome in linear regression model. For the second objective, LC, elevation and NDVI were combined into a single factor consisted of 75 groups and used as determinant where the outcome was LST change. Simple linear regression was used to analyze the relationship of combined factor with LST change.
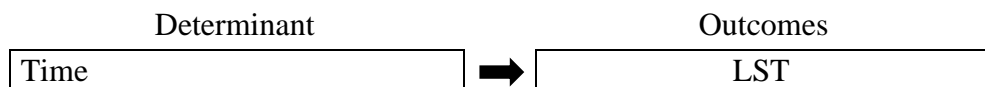
Determinant	Outcomes
Time	LST

Figure 2.9 Diagram of path analysis for objective 1 of the study

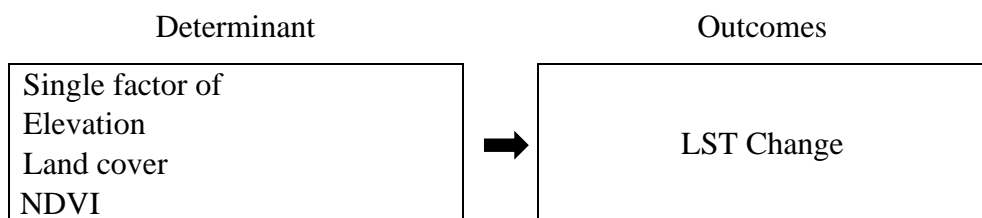| Determinant	Outcomes
Single factor of Elevation Land cover NDVI	LST Change

Figure 2.10 Diagram of path analysis for objective 2 of the study

2.5   Statistical methods

2.5.1 *Descriptive analysis*

After the data has been collected, the first important step is descriptive analysis. This phase entailed giving a data result that could be quantified. The analysis also provided a short overview as well as an idea of the distribution. The frequency and percentage in each category were calculated and displayed on the frequency table and mapping area. In addition, some tiny categories were merged to create enough data for further statistical analysis.

2.5.2 *Autoregressive Integrated Moving Average (ARIMA)*

Based on historical data from previous time points recorded observations, ARIMA models are used to forecast the observation at (t+1). It is necessary to ensure that the time series is stationary over the observation period's historical data. If the time series is not stationary, the records should be handled as a separate factor. Before we move any further, it's crucial to point out that ARIMA is based on the ACF, PACF, AR, MA, and ARMA models.

The Auto Correlation Function (ACF) considers all previous observations, regardless of their impact on the upcoming or current time period. It determines the relationship among time periods t and $(t - k)$. It covers all lags among the time periods t and $(t - k)$. When calculating correlation, the Pearson correlation formula is always utilized. The partial correlation between time periods t and t-k is clarified using the Partial Auto-Correlation Function (PACF). It doesn't account for all the differences in time between t and $t - k$.

In the AR (Autoregressive) model, the time at t is influenced by the observations at various slots $t - 1, t - 2, t - 3, \ldots, t - k$. The coefficient factor determines the influence of previous time spots at that particular point in time. Prior values in the time series may have an impact on the value. AR is a form of model that estimates current or future values in a series by calculating the regression of past time series. If the PACF

of any single lag is more than a significant value, just those data were considered for the model analysis.

Unexpected external factors at various slots $t-1, t-2, t-3, \ldots, t-k$ in the MA (Moving Average) model influence the time period at t. These unforeseen impacts are referred to as errors or residuals. The coefficient factor determines the influence of previous time spots at that particular point in time. A corporate merger or shutdown, for example, can have an impact on the time series value. The MA model determines the current or future values in a series by calculating the residuals or errors of previous time series. All of the lags' ACF values were determined in the time series. If the ACF of any single lag is more than a significant value, just those data will be used for the model analysis.

The ARMA (Auto Regressive Moving Average) model is a cross between the AR and the MA models. This model incorporates the impact of previous lags as well as residuals when forecasting future values of the time series. The AR model's coefficients are represented by while the MA model's coefficients are represented by β.

According to (Kalpakis et al., 2001), ARIMA (p, d, q) is the Box-Jenkins seasonal model, where p and q are the AR and MA component orders, respectively, and d is the differencing order. Some special cases of the ARIMA(p, d, q) model are as follows: AR (p) model is given as ARIMA$(1,0,0)$; MA (q) model is given as ARIMA $(0,0,1)$; ARMA(p, q) model is a combination of the stationary AR(p) and MA(q) models. In this study, ARIMA is applied to indicate that the autocorrelation of LST-day data had been removed in a cubic spline process.

2.5.3 *Cubic spline*

The seasonal trend of LST is investigated using a cubic spline. With errors based on the second derivative, the cubic spline is very trustworthy. According to Wongsai *et al.* (2017), MODIS LST values were gathered over a period of time and changed during the season. The seasonal pattern is thought to be consistent year after year, and other elements like as the LC change, which has a impact on the LST data, are also seen to be steady. Natural disasters that could cause an abrupt shift in data behavior, such as

forest fires, landslides, or tsunamis, were omitted from the study. In an ideal world, the model would offer each day of the year with a year-long seasonal pattern. Based on these considerations, the best model looks to be a cubic spline with exact boundary restrictions that ensure smooth periodicity. When smoothing the spline curve, it's critical to choose the proper placement and amount of parameter knots. However, there are existing optimal parameter selection algorithms depending on how to add knots in intervals where residuals show trends as indicated by autocorrelation or intervals where residuals are inadmissibly significant (Wold, 1974).

The least integrated squared second derivative of all functions is a spline function, which is a piecewise cubic polynomial with continuous second derivatives. A piecewise polynomial of degree k that is continuously differentiable $k-1$ times is referred to as a spline. In the sense that it has less of a tendency to bounce between data points, it is significantly "stiffer" than a polynomial.

Piece-wise interpolation eliminates excessive oscillations and non-convergence by fitting a large number of data points with low-degree polynomials. For example, given a collection of data points, each interval uses a different polynomial to interpolate various interpolants at subsequent times. The successive points are abscissas at which the interpolant switches from one polynomial to another, such as knots (k), breakpoints, or control points. The slopes at subsequent knots should be the same when fitting the seasonal pattern.

The linear least squares regression method can also be used to fit it well. We assume that the end of any year is followed by the start of the next year when fitting the model to time series data, hence the model should be a smooth periodic function with a period of one year (Wongsai et al., 2017). These statements demonstrate that a natural cubic spline with smooth periodic boundary conditions is the optimal model. To fit a smooth spline curve on the display, the number of knots and their locations were calculated through trial and error. A cubic spline function's formula was derived from (Wongsai et al., 2017).

2.5.4 *Simple linear regression*

Simple linear regression was used to determine the LST change caused by the cubic spline. A single predictor was created by combining the LC, elevation, and NDVI. The association between LST change and determinants was determined using simple linear regression. The r-square was used to determine the goodness of fit (Tongkumchum and McNeil, 2009; Venables and Ripley, 2002). For comparing the adjusted LST change within each factor to the overall mean, sum contrasts were utilized and confidence intervals were generated. The R program was used to construct all of the statistical analysis and graphs.

Chapter 3

Results

3.1 Descriptive analysis

Descriptive examination had been conducted for each LC, elevation, and NDVI categories. Fifteen land covers in Sumatra Island were categorized and shown in Figure 3.1. Figure 3.1 shows that mostly Sumatra Island was covered by evergreen broadleaf, forest (44.6%) and woody savannas (33.8%). The urban area only covered 0.51% of the whole Sumatra Island.
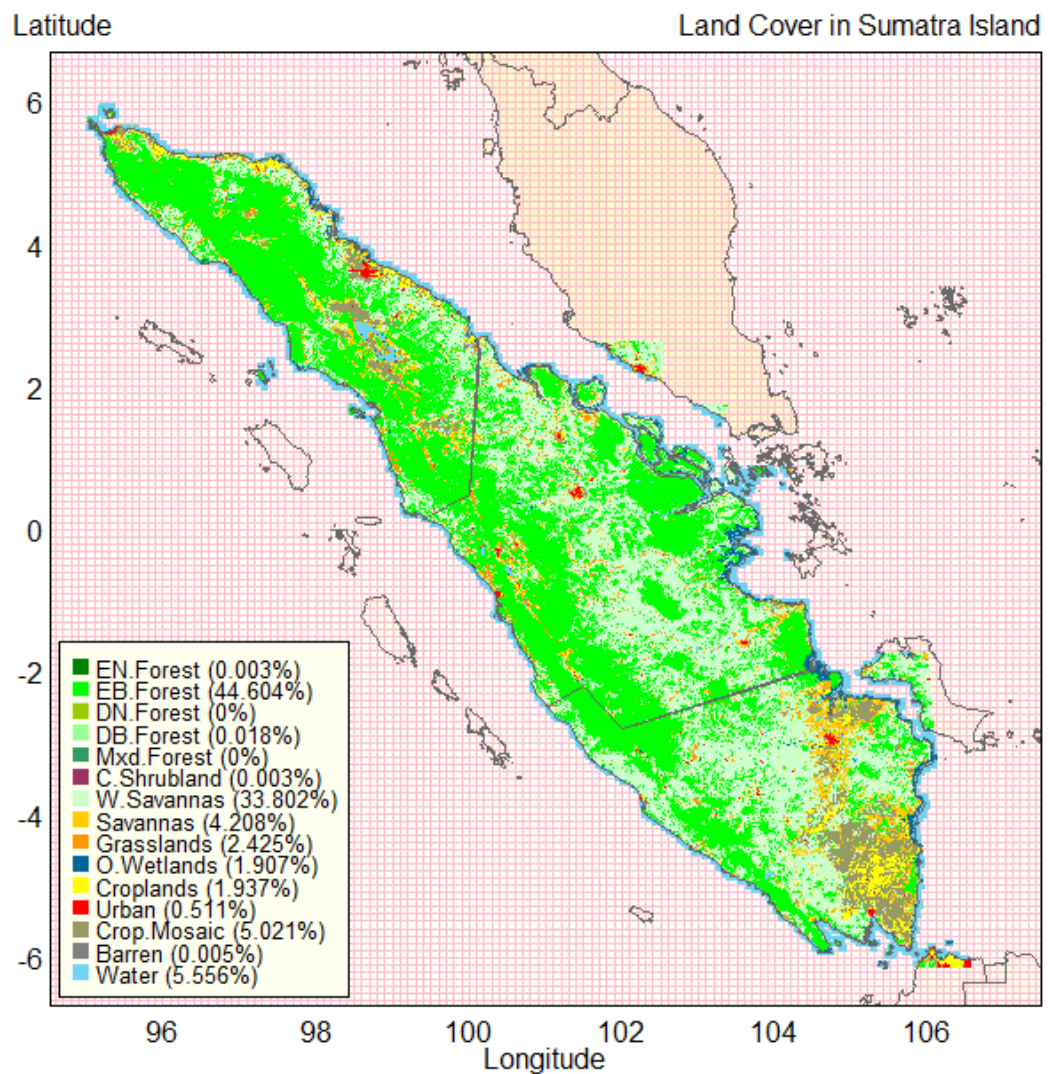

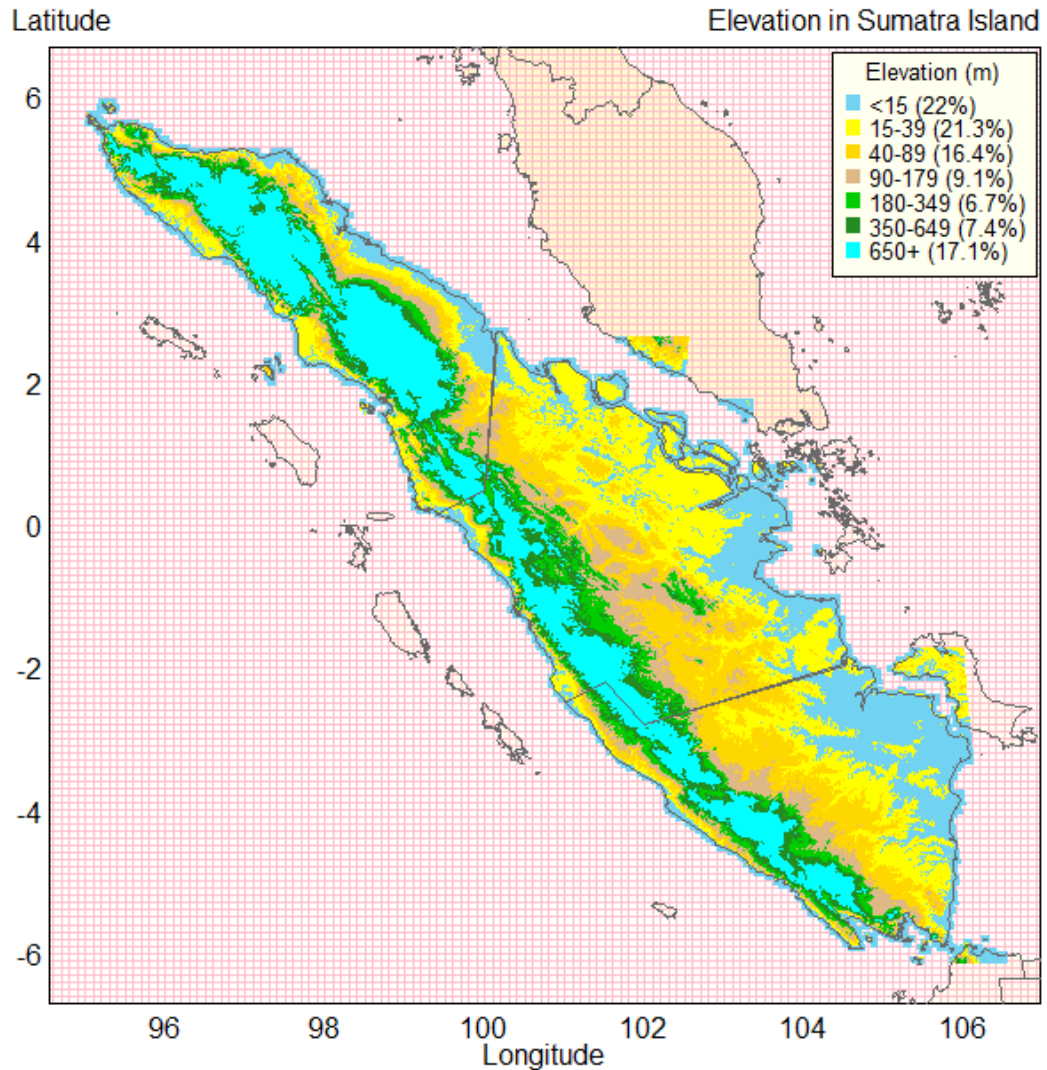Figure 3.1 Land cover in Sumatra Island

Figure 3.2 Elevation of Sumatra Island

The elevation description of Sumatra Island is shown in Figure 3.2. Figure 3.2 implied that 22% Sumatra Island topography was in 15 MASL and 21.3% in 15-39 MASL. Area that has more than 650 MASL was about 17% of the whole Sumatra Island. Based on elevation, LC and NDVI, the distribution of the land area studied in Sumatra is shown in Table 3.1. The largest area (22%) was found between 0 and 14 MASL, while the smallest area was found between 180 and 349 MASL (6.70 %). The highest and lowest areas for land cover were 47.06 % for Evergreen Broadleaf Forest and 0.53 % for urban, correspondingly, while the highest and lowest percentages for NDVI were 54.99 % for category B (0.75-0.8) and 9.24 % for category C (>0.8-1).

Table 3.1 Frequency (pixels) of LC, elevation, and NDVI in Sumatra

Variable	Frequency (pixels)	Percentage (%)
Elevation (meters above sea level)		
0-14	113.748	22.00
15-39	110.129	21.30
40-89	84.794	16.40
90-179	47.050	9.10
180-349	34.641	6.70
350-649	38.261	7.40
650+	88.413	17.10
Land-Cover		
Evergreen Broadleaf Forest	243.339	47.06
Woody Savannas	184.267	35.64
Savannas	22.897	4.43
Grasslands	13.146	2.54
Permanent Wetlands	8.900	1.72
Croplands	10.629	2.06
Urban	2.747	0.53
Cropland or natural vegetation mosaic (Crop.Mos)	27.590	5.34
Water	3.521	0.68
NDVI pattern		
A: < 0.75	184.968	35.77
B: 0.75 - 0.8	284.313	54.99
C: 0.8 – 1	47.755	9.24

3.2 Results of Cubic Spline

LST day data in each super region using cubic spline determined the seasonal patterns and trends using time series dataset. Figure 3.3 and 3.4 show daily and annually LST for region 25 in super region 1 where both figures depict distribution of records. The increasing LST-day trend results from super region 1 were plotted and showed in Figure 3.3. It showed that in a decade this area was getting cooler where the spline indicated minus value. After analyzing for 70 super regions, the results of p value and R^2 were displayed in Figure 3.4 and 3.5.
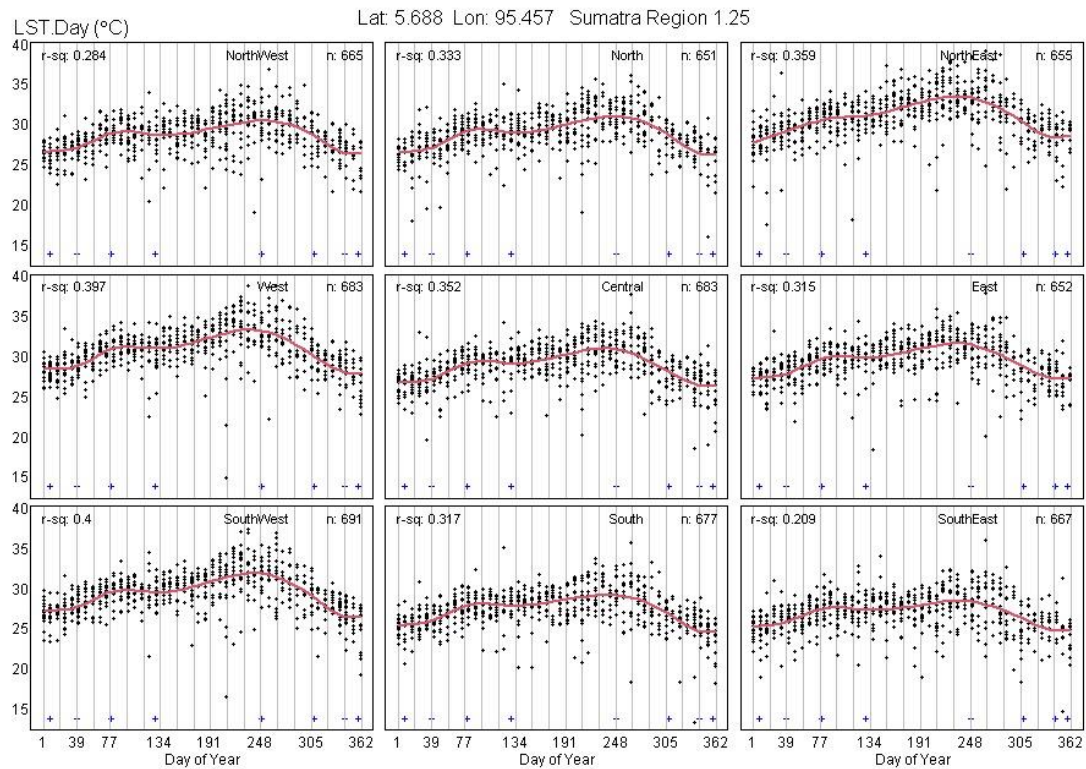
Figure 3.3 Daily LST – Day (°C) in Sumatra 2000-2018 of Super Region 1, region 25

Figure 3.3 visualizes the distribution of daily records in 19 years that mean every scale in X-axis has 19 dots representing each year (if there are no missing values on it). According to Figure 3.3, daily seasonal trend for LST-day (°C) had low variations. The highest LST-day in all areas of region 1 super region 26 happened on day 39 to day 77 (February – April) and day 229 to day 267 (July – September). LST-day trends rose at the beginning of the year and decreased at the end.

Figure 3.4 consists of nine plots where each plot represents one center of the region and eight points of the compass (northwest, west, southwest, north, south, northeast, east, and southeast). Each point of the compass was represented by a different color. Figure 3.4 also shows the outlier values with the purple dot. AR_1 (ARIMA coefficient) is also shown in this figure while the east and southeast region has a very low coefficient value. The number (n) of observations from 2000-2018 was different in each sub-region due to the missing data (cloudcover). Figure 3. 4 indicated that on average the lowest LST-day increase/decade was in the northeast sub-region and the lowest LST-day increase/decade was in the south sub-region.
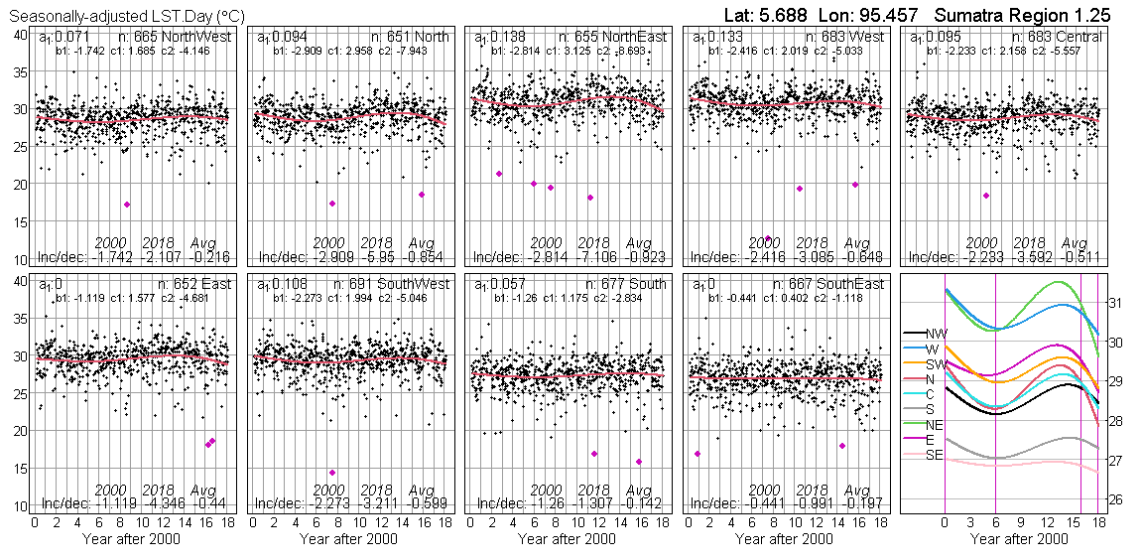
Figure 3.4 Seasonally-adjusted LST – day (°C) in Sumatra 2000-2018

The lowest knots, the lowest p-values, and the highest R^2 were selected to plot on the map as depicted in Figure 3.5. Furthermore, Figure 3.6 shows the map plots of LST-day changing trend in Sumatra 2000-2018. Overall p-value (0.086) and R^2 (0,71%) are shown in the Figure 3.5. LST-day increase/decade by spline model was -0.321 °C.
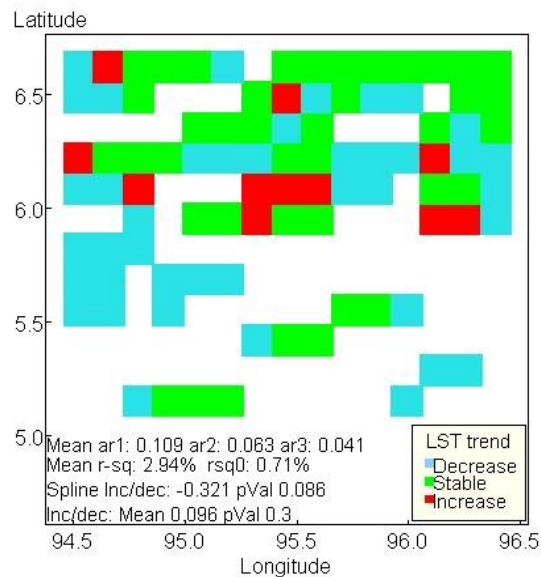

Figure 3.5 Plot of LST-day trend for super region 1

The cubic spline with 8 knots gives the highest average R^2 as shown in Figure 3.3. The highest R^2 is the criteria for deciding the best model.
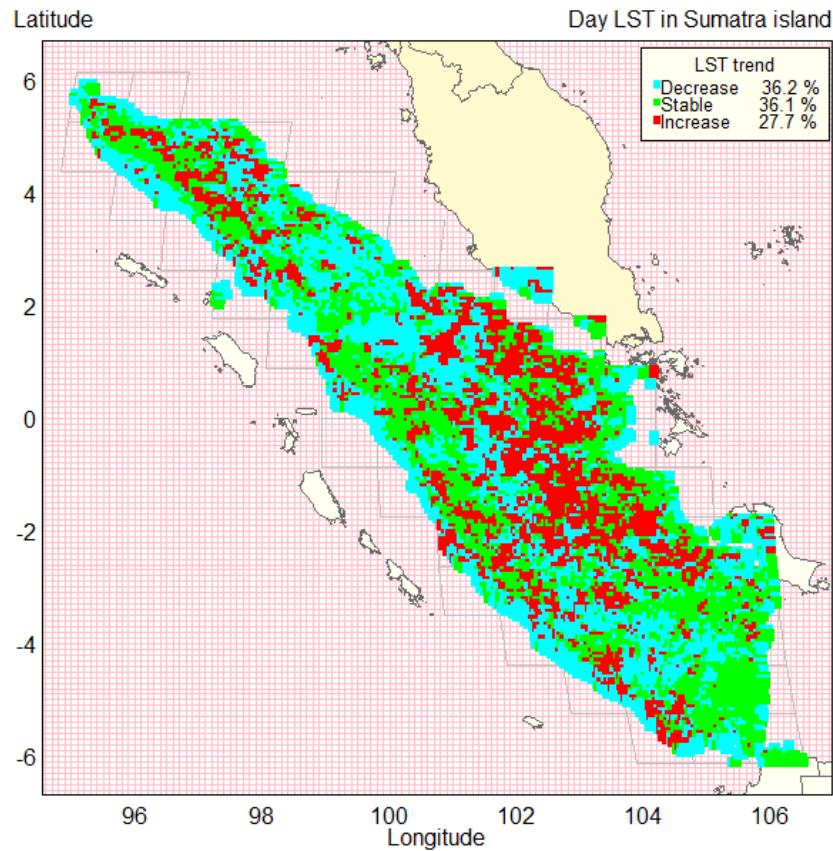
Figure 3.6 LST day–changing trend by cubic spline model in Sumatra 2000-2018

Figure 3.6 represents the LST day change based on a cubic spline results which was a prediction from time series data since 2000-2018. Increasing temperature (red area) occurred in many areas on the island of Sumatra and decreasing temperature (blue area) occurred in some areas as well, and stable temperature occurred in some areas (Green area).

Table 3.2 depicts the rise in daily mean LST change for the three NDVI categories as a function of elevation and LC. Within the evolving NDVI classification, the highest increase was observed in savanna regions with elevation above 320 MASL. The EB. Forest regions with elevation at 60-109 MASL within the NDVI 0.75 classification had the largest decrease in mean LST. The overall mean of LST change in Sumatra had decreased by -0.122 °C/decade, which was utilized in the development of a linear regression model (horizontal red line in Figure 3.8). At an elevation above 320 MASL, the largest increase in LST (1.07 °C/decade) occurred in the savanna.

Table 3. 2 Change in mean LST by NDVI, elevation, and LC in Sumatra

| Categories	NDVI < 0.75	NDVI 0.75- 0.8	NDVI 0.8 - 1
Evergreen Broadleaf Forest			
0-14 MASL			
15-19 MASL	-0.31	-0.10	0.05
20-34 MASL	-0.30	-0.09	0.11
35-59 MASL	-0.20	0.06	0.40
60-109 MASL	-0.54	-0.16	0.19
110-319 MASL	**-0.96**	-0.16	0.02
320-739 MASL	-0.39	-0.18	-0.03
740-1119 MASL	-0.15	-0.14	-0.04
1120+ MASL	-0.01	0.00	0.11
	0.41	0.33	0.45
Woody Savannas			
0-14 MASL	-0.16	-0.09	0.03
15-19 MASL	-0.21	0.00	0.22
20-34 MASL	-0.23	0.07	0.40
35-59 MASL	-0.40	-0.02	0.26
60-109 MASL	-0.54	-0.01	0.18
110-319 MASL	-0.47	-0.14	0.17
320+ MASL	-0.26	-0.18	0.17
Savannas			
0-319 MASL	-0.30	0.04	0.36
320+ MASL	-0.40	0.15	**0.95**
Grasslands	-0.18	0.17	0.69
Permanent Wetlands	-0.40	-0.37	-0.42
Croplands	-0.44	-0.08	-0.02
Urban	0.05	-0.18	-0.15
Cropland or natural vegetation mosaic (Crop Mos)			
0-319 MASL	-0.68	-0.17	0.08
320+ MASL	-0.60	-0.39	-0.42
Water	-0.66	-0.69	-0.82

3.3 Result of simple linear regression
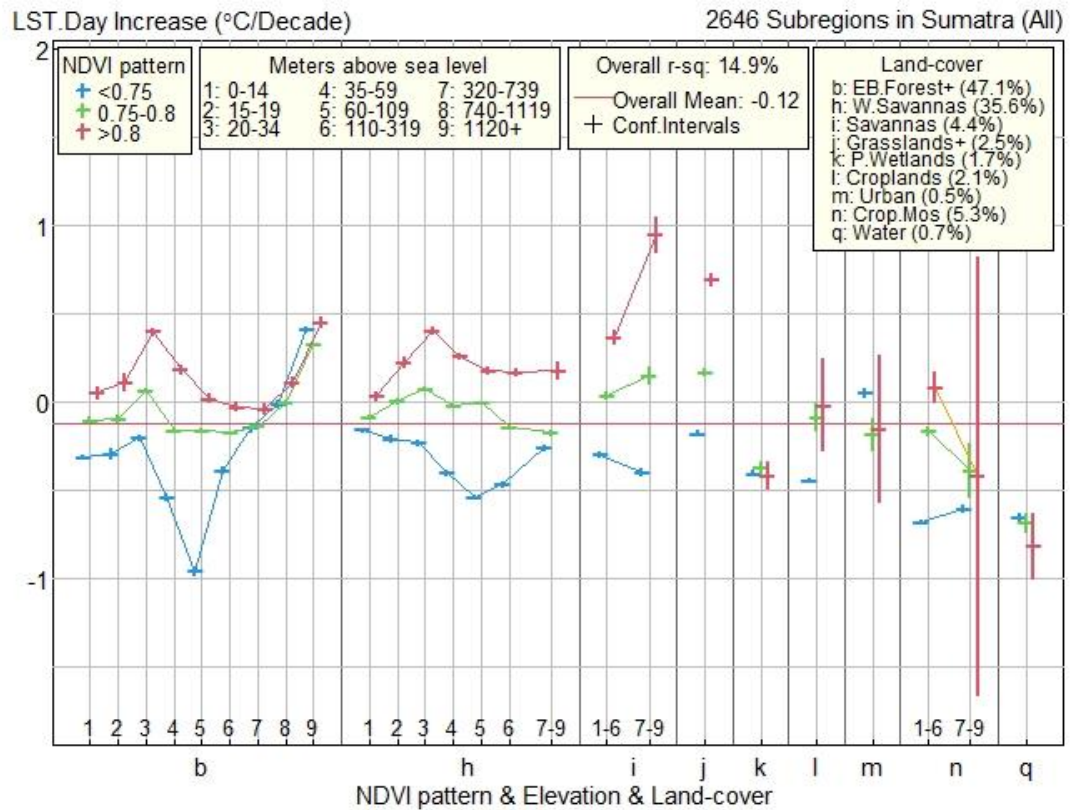
Figure 3.7 Change in daily LST (°C/decade) by NDVI, elevation, and LC of Sumatra

A single factor determinant consisted of 75 groups was used to predict the LST change. The data in Table 3.2 is depicted in Figure 3.7. LST decreased by 0.122 °C on an overall mean per decade. Figure 3.8 shows that in areas of EB forest, which make-up 47.1 percent of Sumatra's land cover, where the NDVI was less than 0.75 and the elevation was 60-109 MASL. The LST had decreased by -0.84 °C per decade. The R^2 in the simple regression generated using the data in Table 3.2 was 0.149, meaning that elevation, LC, and NDVI accounted for just 14.9 percent of the variance in the LST, indicating that other variables accounted for 85.1 percent of the variation.

Chapter 4

Discussion and Conclusions

4.1 Discussion

The highest LST-day occurred between days 39 and 77, and between days 229 and 267, according to the seasonal trend of this study. It indicated that the maximum LST in the whole Sumatra Island occurred at two peaks, one at the beginning of the year and the other at the end of the year. This study also indicated that elevation, LC, and NDVI accounted for just 14.9 percent of the variance in the LST, as the other variables accounted for 85.1 percent of the variation. During the study period, not all parts of Sumatra Island experienced an increase in daily LST. It is determined by biophysical characteristics or other factors in that particular area.

The biophysical and demographic characteristics can determine the seasonal trends in the LST of an area. Referring to a study on the seasonal and interannual variations in the LST, it was stated that forest, agriculture, and water were found as the most significant factors contributing to the LST variations (Gao et al., 2016; Xiao et al., 2008). The other significant factor is the presence of solar radiation. The presence of solar radiation was believed to be the most important factor influencing the LST variations. The more solar radiation absorbed or radiated on the earth's surface, the higher the LST detected (Lindsey, 2009). Since the study's findings indicated that not all areas in Sumatra had increased, there might be other factors considered as contributing factors to the LST variations. The results of this study are also supported by other research which stated that climate change could occur in a regional scale (Bradley and Diaz, 2010). Other studies have also shown that LST variations could also be influenced by other factors such as NDVI, elevation, and land cover (Aik et al., 2020; Gao et al., 2008; Guha et al., 2018)

Various reports indicated that the earth has experienced an increase in temperature globally (Hansen et al., 2010; NASA Earth Observatory, 2016; NOAA NCEI, 2020). This study showed differently by stating that the average LST on the island of Sumatra decreased by -0.122 degrees Celsius per decade. Another study on the island of New

Guinea also showed different results, but it was clear that certain regions had decreased the LST (Munawar et al., 2020). The decrease of the LST is a common phenomenon in the forest land area due to its function as canopies for the land (Bakar et al., 2016; Hua and Ping, 2018). The increase in the LST was also observed in arctic regions, specifically on the island of Spitsbergen (Fitrahanjani et al., 2020). The Sumatra and New Guinea islands are tropical regions that are warm all year and have a rich biodiversity, which can affect changes in the LST (Antão et al., 2019).

While the average LST in Sumatra decreased as compared to New Guinea and Spitsbergen, this study also indicated that the LST rose in some areas. The decrease in the LST could be due to contributing factors such as healthy vegetation and water body. This study found a decline in the LST in the E.B. Forest. The same trend was observed in a study in China, Bangladesh, and Europe in which the lowest LST reduction was observed in areas with body water and E.B. Forest, despite the fact that the LST increased as elevation increased (Schwaab et al., 2020; Tan et al., 2020; Uddin and Mondal, 2020). Land cover in the form of the forest has the property of absorbing solar radiation and tends to provide a cooling effect above the ground (Huryna and Pokorný, 2016) since tall trees provide shade for the soil surface (Lin and Lin, 2010). On the other hand, the warming effect will occur in land cover types other than forest, for example, residential areas or areas with little vegetation (Duveiller et al., 2020).

This study revealed that the highest increase in the LST occurred in savanna areas. The characteristics of savanna are grasslands that have less plant diversity compared to green forests. This type of plant in such areas is low grass in which leaves are small and absorb little solar radiation (Armson, 2012). Too much solar radiation is one contributing reason to the rising temperature of the soil's surface (Wild, 2012). Another study in Australia also showed a similar case that the savanna was projected to experience an increase in temperature (Reside et al., 2012). Savannas, including woody-herbaceous systems, are usually described as a part of more widely distributed 'tree-grass' vegetation communities, and the whole world is covered by savannas and woody savannas by 13.7% (Mildrexler et al., 2011). Trees make greater structural complexity, including the exchange of latent heat, into the savanna environment (Baldocchi et al., 2004). According to a study in the United States, the air temperature potential in

savanna areas was warmer than that of other land types, such as grassland (Baldocchi and Ma, 2013).

When discussing LULC, it should also consider the degree of plant greenness (NDVI) in a region. A previous study in Mexico and Brazil found that increasing land cover areas such as forests or healthy vegetation were more likely to reduce LST (Gomez-Martinez et al., 2021; Wanderley et al., 2019). Many studies have reported that LULC affected LST (Odindi et al., 2015; Rasul et al., 2017). The world will encounter an increase in temperatures if land cover is drastically diminished (Parmesan and Hanley, 2015). The evaporation process allows green trees or other plants that cover the earth surface to absorb heat as a result of solar radiation reflection. The heat on the ground will be metabolized by trees and converted into different types of energy, lowering the temperature on the land surface. This suggests that LULC, like healthy vegetation, doesn't tend to raise LST (Babalola and Akinsanola, 2016).

The decrease in the LST in Sumatra also indicated that the island's vegetation was in a relatively good condition. Although other studies showed high deforestation and land-use change in Sumatra (Austin et al., 2019). The Indonesian government is currently aggressively regulating and protecting forests on the island of Sumatra and other large islands (New York Declaration on Forest, 2019). Deforestation prevention programs and land management can be factors to reduce an increase in the LST in a regional scale (Jaafar et al., 2020; Tacconi et al., 2019).

The elevation is one of the factors that can contribute to the LST. Previous studies in the Horn of Africa and China showed different findings that the LST in high-altitude areas with short vegetation types would decrease (Abera et al., 2019; Peng et al., 2020). Other findings in China showed that higher altitude in areas would decrease the LST steadily (Deng et al., 2018). Different topography is spread across the island of Sumatra and has different types of vegetation. This shows that the elevation and vegetation are very likely related to the LST. A study in Jaipur, India indicates that elevation had a strong relationship with the LST (Khandelwal et al., 2018).

Due to the Sumatra Islands are located between the western Pacific Ocean and the eastern Indian Ocean, the regional climate characteristics over Sumatra Islands are known to have seasonal and inter-annual variability predominantly related to the monsoon, maritime climate, or rainfall pattern, etc. Those factors may affect the LST change.

The current findings provide insights for better understanding of environmental changes, particularly the state of regional climate change related to natural phenomena and anthropogenic activities. Research and development organizations can promote these findings in policymaking and strategic planning processes, for example, planting crops, agricultural expansion, deforestation, and urban heat measures. To enhance the cloud detection algorithm, more future studies should be conducted.

4.2 Conclusions

Little variations were exhibited by daily seasonal trend for LST-day (°C). LST-day was increased at the beginning of the year and decreased at the end of the year. This study finding also mentioned that not all LST in the area of Sumatra Island increased. This study showed that LST variation differs by area, and so additional variables must be explored more to determine the impact of all variables on the LST. Despite the fact that the total LST change in Sumatra, Indonesia, is within a tolerable range (-0.122 °C/decade), the largest increase is 1.07 °C/decade and the greatest decrease is -0.84 °C/decade. Deforestation, which is widespread across Indonesia's big island, may be a significant contributory factor in LST change, necessitating continuous monitoring of LST change across the country.

4.3 Limitation and recommendation

This study demonstrated that LST change was varied in different local scale areas and based on that circumstance. Individual correlation needs to be investigated to look at the relationship of each dependent variable to LST. Global scale of assessment was needed to counter the climate change due to the unwanted effect of it. Further investigation of other predictors is needed to gain information about the increasing LST on a global scale.

References

Abera, T. A., Heiskanen, J., Pellikka, P., Rautiainen, M., & Maeda, E. E. (2019). Clarifying the role of radiative mechanisms in the spatio-temporal changes of land surface temperature across the Horn of Africa. *Remote Sensing of Environment*, *221*, 210–224. https://doi.org/https://doi.org/10.1016/j.rse.2018.11.024

Adeyeri, O., & Okogbue, E. (2014). Effect of Landuse Landcover on Surface Temperature in Abuja Using Remote Sensing and Geographic Information System (Gis). *Proceedings of Climate Change, and Sustainable Economic Development*, *November 2017*, 175–184. https://doi.org/978-978- 521-43-6-9

Aik, D. H. J., Ismail, M. H., & Muharam, F. M. (2020). Land Use/Land Cover Changes and the Relationship with Land Surface Temperature Using Landsat and MODIS Imageries in Cameron Highlands, Malaysia. *Land*, *9*(10), 1–23. https://doi.org/10.3390/land9100372

Alavipanah, S., Wegmann, M., Qureshi, S., Weng, Q., & Koellner, T. (2015). The Role of Vegetation in Mitigating Urban Land Surface Temperatures: A Case Study of Munich, Germany during the Warm Season. *Sustainability*, *7*(4), 4689–4706. https://doi.org/10.3390/su7044689

Antão, L. H., Bates, A. E., Blowes, S. A., Waldock, C., Supp, S. R., Magurran, A. E., Dornelas, M., & Schipper, A. M. (2019). Temperature-related biodiversity change across temperate marine and terrestrial systems. *BioRxiv*, 1–27. https://doi.org/10.1101/841833

Armson, D. (2012). *The Effect of Trees and Grass on the Thermal and Hydrological Performance of an Urban Area*. Faculty of Life Sciences, University of Manchester.

Austin, K. G., Schwantes, A., Gu, Y., & Kasibhatla, P. S. (2019). What causes deforestation in Indonesia? *Environmental Research Letters*, *14*(2). https://doi.org/10.1088/1748-9326/aaf6db

Babalola, O., & Akinsanola, A. (2016). Change Detection in Land Surface Temperature and Land Use Land Cover over Lagos Metropolis, Nigeria. *Journal of Remote Sensing & GIS*, *5*(3), 2–7. https://doi.org/10.4172/2469-

4134.1000171

Bakar, S. B. A., Pradhan, B., Lay, U. S., & Abdullahi, S. (2016). Spatial assessment of land surface temperature and land use/land cover in Langkawi Island. *IOP Conference Series: Earth and Environmental Science*, *37*(1). https://doi.org/10.1088/1755-1315/37/1/012064

Baldocchi, D. D., Xu, L., & Kiang, N. (2004). How plant functional-type, weather, seasonal drought, and soil physical properties alter water and energy fluxes of an oak-grass savanna and an annual grassland. *Agricultural and Forest Meteorology*, *123*(1–2), 13–39. https://doi.org/10.1016/j.agrformet.2003.11.006

Baldocchi, D., & Ma, S. (2013). How will land use affect air temperature in the surface boundary layer? Lessons learned from a comparative study on the energy balance of an oak savanna and annual grassland in California, USA. *Tellus, Series B: Chemical and Physical Meteorology*, *65*(1). https://doi.org/10.3402/tellusb.v65i0.19994

Bottyán, Z., & Unger, J. (2003). A multiple linear statistical model for estimating the mean maximum urban heat island. *Theoretical and Applied Climatology*, *75*(3), 233–243.

Bradley, R. S., & Diaz, H. F. (2010). *Regional-Scale Climate Change: Observations and Model Simulations*.

Chu, D. A., Kaufman, Y. J., Zibordi, G., Chern, J. D., Mao, J., Li, C., & Holben, B. N. (2003). Global monitoring of air pollution over land from the Earth Observing System-Terra Moderate Resolution Imaging Spectroradiometer (MODIS). *Journal of Geophysical Research: Atmospheres*, *108*(21), 1–18. https://doi.org/10.1029/2002jd003179

Chudnovsky, A., Ben-Dor, E., & Saaroni, H. (2004). Diurnal thermal behavior of selected urban objects using remote sensing measurements. *Energy and Buildings*, *36*(11), 1063–1074. https://doi.org/https://doi.org/10.1016/j.enbuild.2004.01.052

Demir, G., & Akyurek, Z. (2016). The Importance of Precise Digital Elevation Models (DEM) in Modelling Floods. *EGU General Assembly Conference Abstracts*, EPSC2016-9604.

Deng, Y., Wang, S., Bai, X., Tian, Y., Wu, L., Xiao, J., Chen, F., & Qian, Q. (2018). Relationship among land surface temperature and LUCC, NDVI in typical karst area. *Scientific Reports*, *8*(1), 1–12. https://doi.org/10.1038/s41598-017-19088-x

Dewan, A. M., Yamaguchi, Y., & Rahman, M. Z. (2012). Dynamics of land use/cover changes and the analysis of landscape fragmentation in Dhaka Metropolitan, Bangladesh. *GeoJournal*, *77*(3), 315–330. https://doi.org/10.1007/s10708-010-9399-x

Dousset, B., & Gourmelon, F. (2003). Satellite multi-sensor data analysis of urban surface temperatures and landcover. *ISPRS Journal of Photogrammetry and Remote Sensing*, *58*(1–2), 43–54.

Duveiller, G., Caporaso, L., Abad-Viñas, R., Perugini, L., Grassi, G., Arneth, A., & Cescatti, A. (2020). Local biophysical effects of land use and land cover change: towards an assessment tool for policy makers. *Land Use Policy*, *91*(August 2018), 104382. https://doi.org/10.1016/j.landusepol.2019.104382

Eliasson, I. (1996). Urban nocturnal temperatures, street geometry and land use. *Atmospheric Environment*, *30*(3), 379–392.

Engel-Cox, J. A., Holloman, C. H., Coutant, B. W., & Hoff, R. M. (2004). Qualitative and quantitative evaluation of MODIS satellite sensor data for regional and urban scale air quality. *Atmospheric Environment*, *38*(16), 2495–2509. https://doi.org/10.1016/j.atmosenv.2004.01.039

Fitrahanjani, C., Prasetya, T. A. E., & Indawati, R. (2020). A statistical method for analysing temperature increase from remote sensing data with application to Spitsbergen Island. *Modeling Earth Systems and Environment*. https://doi.org/10.1007/s40808-020-00907-6

Friedl, M. A., Sulla-menashe, D., Tan, B., Schneider, A., Ramankutty, N., Sibley, A., & Huang, X. (2005). Remote Sensing of Environment MODIS Collection 5 global land cover : Algorithm refinements and characterization of new datasets. *Remote Sensing of Environment*, *114*(1), 168–182. https://doi.org/10.1016/j.rse.2009.08.016

Fu, G., Shen, Z., Zhang, X., Shi, P., Zhang, Y., & Wu, J. (2011). Estimating air temperature of an alpine meadow on the Northern Tibetan Plateau using

MODIS land surface temperature. *Acta Ecologica Sinica*, *31*(1), 8–13. https://doi.org/10.1016/j.chnaes.2010.11.002

Gao, H., Zhang, S., Fu, R., Li, W., & Dickinson, R. E. (2016). Interannual Variation of the Surface Temperature of Tropical Forests from Satellite Observations. *Advances in Meteorology*, *2016*. https://doi.org/10.1155/2016/4741390

Gao, M., Qin, Z., Qiu, J., Liu, S., Xu, B., Li, W., & Yang, X. (2008). *Retrieving spatial-temporal variation of land surface temperature in Tibetan Plateau for the years 2005-2006 from MODIS satellite data*. *7110*(June 2014), 71101A-71101A – 10. https://doi.org/10.1117/12.800098

Gomez-Martinez, F., De Beurs, K. M., Koch, J., & Widener, J. (2021). Multi-temporal land surface temperature and vegetation greenness in urban green spaces of Puebla, Mexico. *Land*, *10*(2), 1–25. https://doi.org/10.3390/land10020155

Guan, Y., Dan, Q., Zhang, C., Cai, D., Xuying, L. I. U., & Shan, Guo. (2014). Urban Surface Energy Distribution and Related Characteristics：An Remote Sensing Based Research Applied to the International Livable Cities. *Journal of Geo-Information Science*, *16*(5), 806-814. https://doi.org/10.3724/SP.J.1047.2014.00806

Guha, S., Govil, H., Dey, A., & Gill, N. (2018). Analytical study of land surface temperature with NDVI and NDBI using Landsat 8 OLI and TIRS data in Florence and Naples city, Italy. *European Journal of Remote Sensing*, *51*(1), 667–678. https://doi.org/10.1080/22797254.2018.1474494

Gupta, P., Christopher, S. A., Wang, J., Gehrig, R., Lee, Y., & Kumar, N. (2006). Satellite remote sensing of particulate matter and air quality assessment over global cities. *Atmospheric Environment*, *40*(30), 5880–5892. https://doi.org/10.1016/j.atmosenv.2006.03.016

Hansen, J., Ruedy, R., Sato, M., & Lo, K. (2010). Global surface temperature change. *Reviews of Geophysics*, *48*(4), 1–29. https://doi.org/10.1029/2010RG000345

Hansen, James, Kharecha, P., Sato, M., Masson-Delmotte, V., Ackerman, F., Beerling, D. J., Hearty, P. J., Hoegh-Guldberg, O., Hsu, S.-L., Parmesan, C., Rockstrom, J., Rohling, E. J., Sachs, J., Smith, P., Steffen, K., Van Susteren, L., von Schuckmann, K., & Zachos, J. C. (2013). Assessing "Dangerous

Climate Change": Required Reduction of Carbon Emissions to Protect Young People, Future Generations and Nature. *PLOS ONE*, *8*(12), e81648.

Howe, C. J., Cole, S. R., Westreich, D. J., Greenland, S., Napravnik, S., & Eron Jr, J. J. (2011). Splines for trend analysis and continuous confounder control. *Epidemiology (Cambridge, Mass.)*, *22*(6), 874.

Hua, A. K., & Ping, O. W. (2018). The influence of land-use/land-cover changes on land surface temperature: a case study of Kuala Lumpur metropolitan city. *European Journal of Remote Sensing*, *51*(1), 1049–1069. https://doi.org/10.1080/22797254.2018.1542976

Huang, R., Zhang, C., Huang, J., Zhu, D., Wang, L., & Liu, J. (2015). Mapping of daily mean air temperature in agricultural regions using daytime and nighttime land surface temperatures derived from TERRA and AQUA MODIS data. *Remote Sensing*, *7*(7), 8728–8756. https://doi.org/10.3390/rs70708728

Huryna, H., & Pokorný, J. (2016). The role of water and vegetation in the distribution of solar energy and local climate: a review. *Folia Geobotanica*, *51*(3), 191–208. https://doi.org/10.1007/s12224-016-9261-0

Hutchison, K. D. (2003). Applications of MODIS satellite data and products for monitoring air quality in the state of Texas. *Atmospheric Environment*, *37*(17), 2403–2412. https://doi.org/10.1016/S1352-2310(03)00128-6

Jaafar, W. S. W. M., Maulud, K. N. A., Muhmad Kamarulzaman, A. M., Raihan, A., Sah, S. M., Ahmad, A., Maizah Saad, S. N., Mohd Azmi, A. T., Syukri, N. K. A. J., & Khan, W. R. (2020). The influence of deforestation on land surface temperature-A case study of Perak and Kedah, Malaysia. *Forests*, *11*(6). https://doi.org/10.3390/F11060670

Justice, C. O., Townshend, J. R. G., Vermote, E. F., Masuoka, E., Wolfe, R. E., Saleous, N., Roy, D. P., & Morisette, J. T. (2002). An overview of MODIS Land data processing and product status. *Remote Sensing of Environment*, *83*(1–2), 3–15. https://doi.org/10.1016/S0034-4257(02)00084-6

Kalpakis, K., Gada, D., & Puttagunta, V. (2001). Distance measures for effective clustering of ARIMA time-series. *Proceedings 2001 IEEE International Conference on Data Mining*, 273–280.

Kaufman, Y. J., & Tanré, D. (1998). Algorithm for remote sensing of tropospheric

aerosol from MODIS. *NASA MODIS Algorithm Theoretical …*, 85.
http://capita.wustl.edu/Capita/CapitaReports/091013_AQRS/AQRS/Particulat
es/Retrieval
Algorithms/ATBDs/MODIS.pdf%5Cnhttp://capita.wustl.edu/CAPITA/capitar
eports/091013_AQRS/AQRS/Particulates/Retrieval
Algorithms/ATBDs/MODIS.pdf

Khandelwal, S., Goyal, R., Kaul, N., & Mathew, A. (2018). Assessment of land
surface temperature variation due to change in elevation of area surrounding
Jaipur, India. *Egyptian Journal of Remote Sensing and Space Science*, *21*(1),
87–94. https://doi.org/10.1016/j.ejrs.2017.01.005

King, M. D., Kaufman, Y. J., Tanré, D., & Nakajima, T. (1999). Remote Sensing of
Tropospheric Aerosols from Space: Past, Present, and Future. *Bulletin of the
American Meteorological Society*, *80*(11), 2229–2259.
https://doi.org/10.1175/1520-0477(1999)080<2229:RSOTAF>2.0.CO;2

Lambin, E. F., Geist, H. J., & Lepers, E. (2003). Dynamics of land-use and land-cover
change in tropical regions. *Annual Review of Environment and Resources*, *28*,
205–241. https://doi.org/10.1146/annurev.energy.28.050302.105459

Li, Y., Zhao, M., Mildrexler, D. J., Motesharrei, S., Mu, Q., Kalnay, E., Zhao, F., Li,
S., & Wang, K. (2016). Potential and actual impacts of deforestation and
afforestation on land surface temperature. *Journal of Geophysical Research*,
121(24), 14372–14386. https://doi.org/10.1002/2016JD024969

Li, Z. L., Tang, B. H., Wu, H., Ren, H., Yan, G., Wan, Z., Trigo, I. F., & Sobrino, J.
A. (2013). Satellite-derived land surface temperature: Current status and
perspectives. *Remote Sensing of Environment*, *131*, 14–37.
https://doi.org/10.1016/j.rse.2012.12.008

Lin, B. S., & Lin, Y. J. (2010). Cooling effect of shade trees with different
characteristics in a subtropical urban park. *HortScience*, *45*(1), 83–86.
https://doi.org/10.21273/hortsci.45.1.83

Lindsey, R. (2009). Climate and Earth ' s Energy Budget. *Earth Observatory*, 1–19.

Lo, C. P., Quattrochi, D. A., & Luvall, J. C. (1997). Application of high-resolution
thermal infrared remote sensing and GIS to assess the urban heat island effect.
International Journal of Remote Sensing, *18*(2), 287–304.

https://doi.org/10.1080/014311697219079

Marjuki, van der Schrier, G., Tank, A. M. G. K., van den Besselaar, E. J. M., Nurhayati, & Swarinoto, Y. S. (2016). Observed trends and variability in climate indices relevant for crop yields in Southeast Asia. *Journal of Climate*, *29*(7), 2651–2669. https://doi.org/10.1175/JCLI-D-14-00574.1

Mcvicar, T. R., & Jupp, L. B. (1998). Under draft bill, EU wants to raise jail time for hackers, botnet operators | Ars Technica. *Agricultural Systems*, *57*(3), 399–468. http://arstechnica.com/tech-policy/2013/06/under-draft-bill-eu-wants-to-raise-jail-time-for-hackers-botnet-operators/

Mildrexler, D. J., Zhao, M., & Running, S. W. (2011). A global comparison between station air temperatures and MODIS land surface temperatures reveals the cooling role of forests. *Journal of Geophysical Research: Biogeosciences*, *116*(3), 1–15. https://doi.org/10.1029/2010JG001486

Munawar, Prasetya, T. A. E., Mcneil, R., & Jani, R. (2020). Pattern and Trend of Land Surface Temperature Change on New Guinea Island. *Pertanika Journal of Science and Technology*, *28*(4), 1517–1529. https://doi.org/https://doi.org/10.47836/pjst.28.4.20

NASA Earth Observatory. (2016). *World of Change : Global Temperatures*.

Näschen, K., Diekkrüger, B., Evers, M., Höllermann, B., Steinbach, S., & Thonfeld, F. (2019). The Impact of Land Use/Land Cover Change (LULCC) on Water Resources in a Tropical Catchment in Tanzania under Different Climate Change Scenarios. *Sustainability (Switzerland)*, *11*(24). https://doi.org/10.3390/su11247083

National Oceanic and Atmospheric Administration National Centers for Environmental Information (NOAA NCEI). (2020). *Assessing the Global Climate in 2019*.

New York Declaration on Forest. (2019). *Indonesia: A sign of hope for reducing deforestation?* (Vol. 14, Issue 2019).

Newbold, T., Hudson, L. N., Arnell, A. P., Contu, S., De Palma, A., Ferrier, S., Hill, S. L. L., Hoskins, A. J., Lysenko, I., & Phillips, H. R. P. (2016). Has land use pushed terrestrial biodiversity beyond the planetary boundary? A global assessment. *Science*, *353*(6296), 288–291.

Oak Ridge National Laboratory Distributed Active Archive Center (ORNL DAAC). (2018). *MODIS and VIIRS Land Products Global Subsetting and Visualization Tool*. ORNL Distributed Active Archive Center. https://doi.org/10.3334/ornldaac/1379

Odindi, J. O., Bangamwabo, V., & Mutanga, O. (2015). Assessing the value of urban green spaces in mitigating multi-seasonal urban heat using MODIS land surface temperature (LST) and landsat 8 data. *International Journal of Environmental Research*, *9*(1), 9–18. https://doi.org/10.22059/ijer.2015.868

Ozyavuz, M., Bilgili, B. C., & Salici, A. (2015). Determination of vegetation changes with NDVI method. *Journal of Environmental Protection and Ecology*, *16*(1), 264–273.

Parmesan, C., & Hanley, M. E. (2015). Plants and climate change: Complexities and surprises. *Annals of Botany*, *116*(6), 849–864. https://doi.org/10.1093/aob/mcv169

Peng, X., Wu, W., Zheng, Y., Sun, J., Hu, T., & Wang, P. (2020). Correlation analysis of land surface temperature and topographic elements in Hangzhou, China. *Scientific Reports*, *10*(1), 1–16. https://doi.org/10.1038/s41598-020-67423-6

Phan, T. N., Kappas, M., & Tran, T. P. (2018). Land Surface Temperature Variation Due to Changes in Elevation in Northwest Vietnam. *Climate*, *6*(28), 1–19. https://doi.org/10.3390/cli6020028

Pribulick, C. E., Foster, L. M., Bearup, L. A., Navarre-Sitchler, A. K., Williams, K. H., Carroll, R. W. H., & Maxwell, R. M. (2016). Contrasting the hydrologic response due to land cover and climate change in a mountain headwaters system. *Ecohydrology*, *9*(8), 1431–1438.

Rasul, A., Balzter, H., Smith, C., Remedios, J., Adamu, B., Sobrino, J., Srivanit, M., & Weng, Q. (2017). A Review on Remote Sensing of Urban Heat and Cool Islands. *Land*, *6*(2), 38. https://doi.org/10.3390/land6020038

Reside, A. E., VanDerWal, J., & Kutt, A. S. (2012). Projected changes in distributions of Australian tropical savanna birds under climate change using three dispersal scenarios. *Ecology and Evolution*, *2*(4), 705–718. https://doi.org/10.1002/ece3.197

Rijal, S., Saleh, M. B., Jaya, I. N. S., & Tiryana, T. (2016). Deforestation Profile of

Regency Level in Sumatra. *International Journal of Sciences: Basic and Applied Research*, *25*(2,), 385–402.

Sabajo, C. R., Maire, G., June, T., Meijide, A., Roupsard, O., & Knohl, A. (2017). Expansion of oil palm and other cash crops causes an increase of the land surface temperature in the Jambi province in Indonesia. *Biogeosciences*, *14*, 4619–4635.

Schwaab, J., Davin, E. L., Bebi, P., Duguay-Tetzlaff, A., Waser, L. T., Haeni, M., & Meier, R. (2020). Increasing the broad-leaved tree fraction in European forests mitigates hot temperature extremes. *Scientific Reports*, *10*(1), 1–9. https://doi.org/10.1038/s41598-020-71055-1

Sharma, I., Tongkumchum, P., & Ueranantasun, A. (2018). Modeling of Land Surface Temperatures to determine temperature patterns and detect their association with altitude in the Kathmandu Valley of Nepal. *Chiang Mai University Journal of Natural Sciences*, *17*(4), 275–288. https://doi.org/10.12982/CMUJNS.2018.0020

Smith Jr., R., Price, J., Howser, L., Tn, N., E, R., & M, J. (1974). A Smoothing Algorithm Using Cubic Spline Functions. *Nasa Tn D-7397*, *February*, 87.

Sobrino, J. A., Oltra-carrió, R., Sòria, G., Jiménez-muñoz, J. C., Franch, B., Hidalgo, V., Mattar, C., Julien, Y., Cuenca, J., Romaguera, M., Gómez, J. A., Miguel, E. De, Bianchi, R., & Paganini, M. (2013). Evaluation of the surface urban heat island effect in the city of Madrid. *International Journal of Remote Sensing*, *34*(9), 3177–3192. https://doi.org/http://dx.doi.org/10.1080/01431161.2012.716548

Srivastava, A. K., Rajeevan, M., & Kshirsagar, S. R. (2009). Development of a high resolution daily gridded temperature data set (1969–2005) for the Indian region. *Atmospheric Science Letters*, *10*(4), 249–254. https://doi.org/https://doi.org/10.1002/asl.232

Stisen, S., Sandholt, I., Nørgaard, A., Fensholt, R., & Eklundh, L. (2007). Estimation of diurnal air temperature using MSG SEVIRI data in West Africa. *Remote Sensing of Environment*, *110*(2), 262–274. https://doi.org/10.1016/j.rse.2007.02.025

Stroppiana, D., Antoninetti, M., & Brivio, P. A. (2014). Seasonality of MODIS LST

over Southern Italy and correlation with land cover, topography and solar radiation. *European Journal of Remote Sensing*, *47*(1), 133–152. https://doi.org/10.5721/EuJRS20144709

Sun, Q., Wu, Z., & Tan, J. (2012). The relationship between land surface temperature and land use/land cover in Guangzhou, China. *Environmental Earth Sciences*, *65*(6), 1687–1694. https://doi.org/10.1007/s12665-011-1145-2

Suwanwong, A., & Kongchouy, N. (2016). Cubic spline regression model and gee for land surface temperature trend using modis in the cloud forest of Khao Nan National Park Southern Thailand during 2000-2015. *Journal of Engineering and Applied Sciences*, *11*(11), 2387–2395. https://doi.org/10.3923/jeasci.2016.2387.2395

Tacconi, L., Rodrigues, R. J., & Maryudi, A. (2019). Law enforcement and deforestation: Lessons for Indonesia from Brazil. *Forest Policy and Economics*, *108*(May), 101943. https://doi.org/10.1016/j.forpol.2019.05.029

Tan, J., Yu, D., Li, Q., Tan, X., & Zhou, W. (2020). Spatial relationship between land-use/land-cover change and land surface temperature in the Dongting Lake area, China. *Scientific Reports*, *10*(1), 1–9. https://doi.org/10.1038/s41598-020-66168-6

Tongkumchum, P., & McNeil, D. (2009). Confidence intervals using contrasts for regression model. *Songklanakarin Journal of Science and Technology*, *31*(2), 151–156.

Uddin, M. J., & Mondal, C. (2020). Effect of Earth Covering and Water Body on Land Surface Temperature (Lst). *Journal of Civil Engineering, Science and Technology*, *11*(1), 45–56. https://doi.org/10.33736/jcest.2065.2020

Venables, W. N., & Ripley, B. D. (2002). Modern applied statistics with S. In *Statistics and computing. New York: Springer*.

Voogt, J. A., & Oke, T. R. (2003). Thermal remote sensing of urban climates. *Remote Sensing of Environment*, *86*(3), 370–384. https://doi.org/10.1016/S0034-4257(03)00079-8

Wahba, G. (1990). *Spline models for observational data*. SIAM.

Wan, Z., Zhang, Y., Zhang, Q., & Li, Z. L. (2004). Quality assessment and validation of the MODIS global land surface temperature. *International Journal of*

Remote Sensing, *25*(1), 261–274.
https://doi.org/10.1080/0143116031000116417

Wan, Zhengming. (2008). New Refinements and Validation of the MODIS Land-Surface Temperature/Emissivity Products. In *Remote Sensing of Environment* (Vol. 140). https://doi.org/10.1016/j.rse.2006.06.026

Wanderley, R. L. N., Domingues, L. M., Joly, C. A., & Da Rocha, H. R. (2019). Relationship between land surface temperature and fraction of anthropized area in the Atlantic forest region, Brazil. *PLoS ONE*, *14*(12), 1–19. https://doi.org/10.1371/journal.pone.0225443

Wang, J., & Christopher, S. A. (2003). Intercomparison between satellite-derived aerosol optical thickness and PM2.5 mass: Implications for air quality studies. *Geophysical Research Letters*, *30*(21), 2–5. https://doi.org/10.1029/2003GL018174

Weng, Q. (2001). A remote sensing?GIS evaluation of urban expansion and its impact on surface temperature in the Zhujiang Delta, China. *International Journal of Remote Sensing*, *22*(10), 1999–2014. https://doi.org/10.1080/713860788

Weng, Qihao, Lu, D., & Schubring, J. (2004). Estimation of land surface temperature–vegetation abundance relationship for urban heat island studies. *Remote Sensing of Environment*, *89*(4), 467–483. https://doi.org/https://doi.org/10.1016/j.rse.2003.11.005

Wheeler, T., & Braun, J. Von. (2013). Climate Change Impacts on Global Food Security. *Science*, *66*(1997), 37–39.

Wild, M. (2012). Solar Radiation Versus Climate Change. In R. A. Meyers (Ed.), *Encyclopedia of Sustainability Science and Technology* (pp. 9731–9740). Springer New York. https://doi.org/10.1007/978-1-4419-0851-3_448

Wold, S. (1974). Spline Functions in Data Analysis. *Technometrics*, *16*(1), 1–11. https://doi.org/10.1080/00401706.1974.10489142

Wongsai, N., Wongsai, S., & Huete, A. R. (2017). Annual seasonality extraction using the cubic spline function and decadal trend in temporal daytime MODIS LST data. *Remote Sensing*, *9*(12). https://doi.org/10.3390/rs9121254

Xiao, R., Weng, Q., Ouyang, Z., Li, W., Schienke, E. W., & Zhang, Z. (2008). Land surface temperature variation and major factors in Beijing, China.

Photogrammetric Engineering and Remote Sensing, *74*(4), 451–461.
https://doi.org/10.14358/PERS.74.4.451

Yunhao, C., Sui, D. Z., Tung, F., & Wen, D. (2007). Fractal analysis of the structure
and dynamics of a satellite-detected urban heat island. *International Journal of Remote Sensing*, *28*(10), 2359–2366.
https://doi.org/10.1080/01431160500315485

Zhang, H., Zhang, F., Ye, M., Che, T., & Zhang, G. (2016). Estimating daily air
temperatures over the Tibetan Plateau by dynamically integrating MODIS
LST data. *Journal of Geophysical Research*, *121*(19), 11425–11441.
https://doi.org/10.1002/2016JD025154

Zhou, W., Qian, Y., Li, X., Li, W., & Han, L. (2014). Relationships between land
cover and the surface urban heat island: Seasonal variability and effects of
spatial and thematic resolution of land cover data on predicting land surface
temperatures. *Landscape Ecology*, *29*(1), 153–167.
https://doi.org/10.1007/s10980-013-9950-5

Appendix

Publication 1

Systematic Measurement of Temperature Change in Sumatra Island: 2000-2019 MODIS Data Study

Tofan Agung Eka Prasetya[1,2], Munawar[1,3], Sarawuth Chesoh[1]*, Apiradee Lim[1] and Don McNeil[1]

[1]Research Methodology, Department of Mathematics and Computer Science, Faculty of Science and Technology, Prince of Songkla University, Pattani Campus, Muang Pattani, 94000 Thailand
[2]Health Department, Faculty of Vocational Studies, Universitas Airlangga, Jl. Dharmawangsa Dalam Selatan No 68, Airlangga, Gubeng, Surabaya, East Java, Indonesia
[3]Statistics Department, Faculty of Mathematics and Science, Syiah Kuala University, Jl. Syech Abd. Rauf, Kopelma Darussalam, Banda Aceh, Aceh 23111, Indonesia
✉ sarawuth.c@psu.ac.th

Abstract: Land surface temperature (LST) is one of the important factors in the physics of land surface processes to ensure the temperature change in the environment. Sumatra is one of the biggest islands in Indonesia that is suffering from deforestation. The objective of this study was to determine LST changes in Sumatra Island from 2000-2019. LST-day data for each region of Sumatra island were analyzed with cubic spline to see the seasonal pattern and get the LST changing value. The highest LST-day change was in the central region of Sumatra Island which was 0.3842 °C/decade (Z: 8.51, 95% CI: 0.296, 0.473). The lowest LST-day change was in the central north region of Sumatra Island which was –0.1574 °C/decade (Z: –3.022, 95% CI: –0.2596, –0.055). The overall LST-day change was 0.1621 °C/decade (95%CI: 0.1004 - 0.2238).

Keywords: Land surface temperature; Sumatra; Climate change.

Introduction

Global warming is one issue that everyone is talking about recently. As a global issue, the evidence of global warming also needs to be proven by measuring the temperature change in the local and global scales area (Masson-Delmotte et al., 2019). The economy and social life are affected by climate change (Mishra et al., 2010). Further more, climate change has an impact on the environmental and health system (Marjuki et al., 2016; Mboera et al., 2011).

There was evidence that climate change gives an impact or relation to human vulnerability on diseases (Wu et al., 2016). Land Surface Temperature (LST)

plays an important part in monitoring climatological processes at regional to global scales (Li et al., 2013; Wongsai et al., 2017). The measurement of climatic change by LST on a local scale was so critical and commonly used (Luintel et al., 2019). LST is the temperature at the surface layer of land that measures between the atmosphere and material at the soil surface (Stroppiana et al., 2014). The most widely used LST data were the product of a moderate resolution imaging spectroradiometer (MODIS) where the source of the data was from NASA Earth Observation System (EOS) satellites Terra and Aqua, launched in 1999 and 2002 (Wongsai et al., 2017). The satellite sensors will assess LST four times a day. For Terra satellite, the first

*Corresponding Author

assessment was at 10:30 and the second was at 22.30. Then, for Aqua satellite, the third was at 13:30, and the fourth was at 1:30. The data were in daily, eight-day and monthly LST data time series at two spatial resolutions (1 km and 0.05 deg. Climate model grids, CMG) (Wan et al., 2015).

The scientists stated that the world is warming (Arneth et al., 2019). On the other hand, a study was mitigated about the climate change in Southeast Asia, and it was predicted that the temperatures will fall 0.79 to 0.71°C in 2060 (Rasiah et al., 2018). A statement about warming or cooling in the large area was still arguable. Several factors were also thought to be the cause of the warming in a particular area such as the change in land cover, the alterations in forest function, and the increase in human and industrial populations (Longobardi et al., 2016).

Forest existences were the influence of the island temperature on a regional or global scale (Vadrevu et al., 2019). Sumatra Island was the largest of three islands that faced deforestation in Indonesia (Rijal et al., 2016). Forest conversion and climate change issues have fascinated the researchers all around the world (Brack, 2019). Thus, this study chooses Sumatra as an area of the study to measure the LST change in the regional area.

Materials and Methods

Study Area

This study was conducted in Sumatra Island. Sumatra Island is located from east longitude 95 to 106.20 east longitude and north latitude 6.0 to 6.20 south latitude (Figure 1). Forty-five subregions as a sample set were chosen to measure the LST change for Sumatra and were grouped into five regions.

As the pixel was the smallest information from an image, Terra Satellites used an area of 1 km × 1 km as the centre point to build a 3 km (above and below) × 3 km (left and right) and 7 km × 7 km dimensions as the result. This was also a consideration due to the sub-set order recommendation provided by MODIS, and it might hinder the spatial autocorrelation.

The sample points are located around parallels of latitude 105 pixels widths (95 km) apart. We assumed that the nine subregions in one region have the same parameter as in the nine subregions of the other regions, each comprising 49 pixels in a 7 × 7 array, covering the Sumatra island. We specify the latitude and longitude of its central pixel to download data for a subregion.
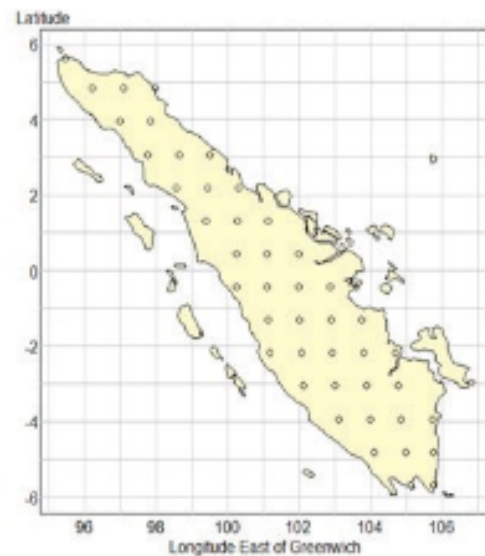

Figure 1: Sumatra area of study.

Data Source and Analysis

Data on daily LST on Sumatra island from March 2000 to November 2019 were used to investigate the change of daily LST. The LST data were freely downloadable from the MODIS database that contains average temperatures every eight days of clear sky for pixels each of area 0.859 km². The time-series trends and patterns of LST were analyzed using a cubic spline. The ARIMA models were used to analyze the time-series data and forecast the LST data, and the multivariate regression models were utilized to minimize the spatial and autocorrelation that was discovered in the ARIMA models.

LST data were the data from freely data sets of MODIS (https://modis.ornl.gov) (ORNL DAAC, 2018; Phan et al., 2018; Wan, 2008). The calculation of the exact location on Latitude and Longitude which is determined or converted by the Modland tile calculator tool in vertical tile, horizontal tile, line, and the sample must be completed to get the LST data. Without the correct and exact location in Latitude and Longitude, the page will not continue or will serve unneeded data. The range between the sample should be at the same range to decrease the spatial correlation.

MOD11A2 Terra LST data were the code for LST data on the next page of the website. Due to land climate components influenced by atmospheric and land processes, these data were only for land, and the area

with water body (ocean) was not available (Luintel et al., 2019; Wan et al., 2015). The analysis of this study was conducted with the R program (Team, 2018). The website give the resume of data that we downloaded, and choose the order, so the data set link is sent to our registered email. LST data must be ordered at a different time because the website only gave one option name of data in each order.

The data access order were sent into an email, and the data were provided in CSV format. The last step is processing and analyzing the data with the R program (Phan et al., 2018; Wan, 2008). LST data were from MODIS 8 days Tera LST (MOD11A2) at 0.05° spatial resolution. The original LST degree measurement was Kelvin which was then converted into Celsius.

After converting the data and managing the year form, we plotted the day temperatures in subregions with fitted cubic splines to see the trends of LST daily for a year from 2000-2019. We assumed that each subregion has constant seasonal variations and seasonal patterns for each day of the year within a year presented in a plot. Running a plot with a natural cubic spline is considered the most appropriate model that ensures the smooth periodicity. With natural cubic splines, one constructs a spline basis with knots at a fixed location throughout the data points (Yang et al., 2012). Choosing the location and number of parameter knots for smoothing the spline curve is a critical issue. Here, we used three models: linear, 4-knots spline, and 7-knots spline. Spline-smoothed seasonal patterns were subtracted to create a season-adjusted time series while using the autoregression model to estimate model curves adjusted for time series correlation.

Linear models were used to show variations and natural cubic splines to identify the seasonal patterns in LST during 2000-2019. The other way, multivariate regression models accommodate temporal and spatial variations in the effects of the covariates, including the intercept (Gamerman and Moreira, 2004). The variance-covariance matrix in multivariate regression is used to create confidence intervals of response variables in linear combinations. The increase in °C per decade will be estimated using the multivariate regression model.

We did not only calculate the LST-day increase in the region but also the Z score to see the LST-day change in sub-region. The increased category of sub-region was divided into five: increase with $z > 1.96$ (red), likely increase with $z > 1$ (orange), stable with $|z| \leq 1$ (green), likely decrease with $z \leq 1$ (ocean boat blue) and decrease with $z < 1.96$ (vivid blue). The regions were grouped in five which is increase (deep pink), likely increase (pink),

stable (vivid green), likely decrease (vivid cyan) and decrease (dark cyan). This shaded group was made to differentiate when depicting the plotting result.

Results and Discussion

Figure 2 depicts the LST change for 45 sub-regions (circle) and five regions (five shaded areas) in Sumatra Island. The day of LST is changed differently in the five regions: decreasing in the central north, increasing in the north, central, central south, and likely increasing in the south. This result was based on Table 1. Table 1 depicts 45 subregions LST day increase from 2000-2019. The plot of LST change for each sub-region was based on this result. The plot of LST change for each region was based on Table 2.

Table 1 depicts that the highest LST day change occurred in sub-region 22 (1.114 °C/decade). The lowest LST day change occurred in sub-region 14 (−1.561 °C/decade). The highest LST day change was in region 3 (central) and the lowest was in region 2 (central).

Table 2 depicts that the highest LST change was in the central region of Sumatra island with a value of 0.3842 °C/decade and Z value of 8.510 (95% CI 0.2957-0.4727). The lowest LST change was in the central north of Sumatra island with a value of −0.1574 °C/decade and Z value of −3.022 (95% CI −0.2596 - −0.0553). The overall average was shown that the LST in Sumatra island was increasing 0.1621 °C/decade and, by using

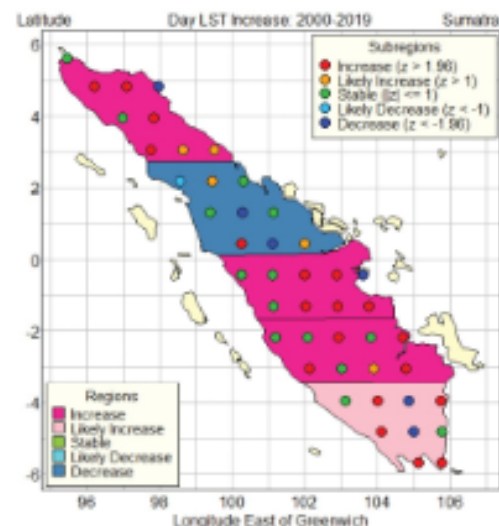**Figure 2:** LST day increase (°C/decade) 2000-2019 of Sumatra.

4   Tofan Agung Eka Prasetya et al.

Table 1: The mean of LST day increase/decade and *p*-value for 45 sub-regions Sumatra island 2000-2019

Sub-reg	Increase	p-value	Sub-reg	Increase	p-value	Sub-reg	Increase	p-value
1	-0.192	0.242	16	0.334	0.025	31	0.066	0.677
2	0.342	0.026	17	-0.579	0	32	0.886	0
3	0.641	0	18	0.314	0.075	33	0.358	0.004
4	-0.334	0.044	19	0.1	0.536	34	0.055	0.681
5	0.177	0.189	20	0.196	0.228	35	0.207	0.11
6	0.297	0.025	21	1.036	0	36	0.41	0.009
7	0.314	0.03	22	1.114	0	37	-0.113	0.388
8	0.363	0.05	23	-0.892	0	38	0.304	0.046
9	0.221	0.143	24	0.134	0.329	39	-0.711	0
10	-0.239	0.091	25	0.371	0.015	40	0.517	0
11	0.307	0.108	26	0.583	0	41	0.383	0.01
12	-0.176	0.483	27	0.678	0	42	-0.575	0.001
13	0.114	0.495	28	-0.083	0.449	43	0.213	0.254
14	-1.561	0	29	0.181	0.179	44	0.406	0.012
15	0.031	0.855	30	0.496	0.001	45	0.345	0.041

Table 2: LST day increase °C/decade and *p*-value for 45 sub-regions Sumatra island 2000-2019

Region	Increase	95% CI (Confident Interval)	Z
North	0.2084	0.1093 - 0.3075	4.123
Central north	-0.1574	-0.2596 - -0.0553	-3.022
Central	0.3842	0.2957 - 0.4727	8.510
Central south	0.2868	0.1971 - 0.3766	6.267
South	0.0885	-0.0283 - 0.2053	1.190
All region average	0.1621	0.1004 - 0.2238	

multivariate analysis, the z-value was 3.4136 (95% CI 0.1004-0.2238).

Figure 3 is a description of Table 2. This figure depicts that the LST day in four regions (North, central, central south and south) was increasing; only
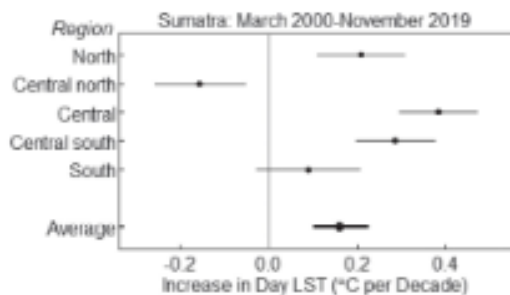
Figure 3: The Sumatra Island increase in Day LST confidence interval.

one region (central north) was decreasing and the overall Sumatra island was increasing. A study shows that the deforestation in Sumatra was statistically increasing (Basyuni et al., 2018). The area of central Sumatra island was the most deforested area (Poor et al., 2019). This can be evidence that the occurrence of deforestation was considered affecting the increase of temperature ambient.

Cooling and increasing temperatures in an area and the factors that cause it is still a matter of debate (Easterling and Wehner, 2009; Neukom et al., 2019). A study states that the cause of a temperature increase in an area was due to changes in land cover, gas emissions, and an increase in human and industrial populations (Datta et al., 2017).

The previous study shows that the Sumatra area's surface temperatures have increased and this confirms the findings of this study (Musyayyadah and Vonnisa, 2019). This warming condition can be triggered by

several causes such as land cover changes (Mitraka and Chrysoulakis, 2016; Saputra and Lee, 2019). Land cover in Sumatra is a largely tropical rainforest and currently is experiencing massive deforestation (Goetz et al., 2012; Rijal et al., 2016; Saputra and Lee, 2019). Forest conversion can cause an increase in the temperature in the local region (Prevedello et al., 2019).

A temperature increase also occurred in areas with a small vegetation index (Sun et al., 2012). Area with small vegetation index (unhealthy vegetation area) or converted land cover area also affects LST change (Deng et al., 2018). A study illustrates that a low NDVI (Normalized different vegetation index) will result in a high LST (Rahmad et al., 2019). Contrarywise, if the NDVI was high, the LST tends to be low (Parveen and Ghaffar, 2019). These findings occur in the central part of the North Sumatra region.

Temperature changes that occur in Sumatra are still relatively small. A study shows that the increase in temperature of an area can be reduced if the converted-LULC (Land Use-Land Cover) area can be recuperated as formerly (forest) (Gogoi et al., 2019). It was expected that an LST increase can be affected or reduced by increasing NDVI (Cooper et al., 2017).

Conclusions

The increase in LST in Sumatra confirms that global warming is occurring in the local area (an island) of Sumatra. LST on Sumatra island was increasing 0.1621 °C/decade in the whole island (45 sub-regions and five regions). Further studies on a broader scale are urgently needed since this study only discovered the cooling phenomenon. Other factors such as land use-land cover (LULC) and NDVI can be taken into consideration for further studies. It will be a good issue to investigate the factor that affects the LST change.

Acknowledgements

References

Arneth, A., Barbosa, H., Benton, T., Calvin, K., Calvo, E., Connors, S. and Cowie, A., 2019. Climate Change and Land. *In:* Intergovernmental Panel on Climate Change.

Basyuni, M., Sulistiyono, N., Wati, R. and Hayati, R., 2018. Deforestation trend in North Sumatra over 1990-2015. *IOP Conference Series: Earth and Environmental Science,* **122(1)**. https://doi.org/10.1088/1755-1315/122/1/012059

Brack, D., 2019. Forests and Climate Change Duncan Brack *In:* The fourteenth session of the United Nations Forum on Forests. Retrieved from https://www.un.org/esa/forests/wp-content/uploads/2019/03/UNFF14-BkgdStudy-SDG13-March2019.pdf

Cooper, L.A., Ballantyne, A.P., Holden, Z.A. and Landguth, E.L., 2017. Disturbance impacts on land surface temperature and gross primary productivity in the western United States. *Journal of Geophysical Research: Biogeosciences,* **122(4)**: 930-946. https://doi.org/10.1002/2016JG003622

Datta, D., Prasad, M. and Mandla, V.R., 2017. Study of various factors influence on land surface temperature in urban environment. *Journal of Urban and Environmental Engineering,* **11(1)**: 58-62. https://doi.org/10.4090/juee.2017.v11n1.058062

Deng, Y., Wang, S., Bai, X., Tian, Y., Wu, L., Xiao, J., … Qian, Q., 2018. Relationship among land surface temperature and LUCC, NDVI in typical karst area. *Scientific Reports,* **8(1)**: 1-12. https://doi.org/10.1038/s41598-017-19088-x

Easterling, D.R. and Wehner, M.F., 2009. Is the climate warming or cooling? *Geophysical Research Letters,* **36(8)**: 4-6. https://doi.org/10.1029/2009GL037810

Gamerman, D. and Moreira, A.R.B., 2004. Multivariate spatial regression models. *Journal of Multivariate Analysis,* **91(2)**: 262-281. https://doi.org/10.1016/j.jmva.2004.02.016

Goetz, S., Hansen, M.C., Baccini, A., Tyukavina, A., Potapov, P., Margono, B.A., … Turubanova, S., 2012. Mapping and monitoring deforestation and forest degradation in Sumatra (Indonesia) using Landsat time series data sets from 1990 to 2010. *Environmental Research Letters,* **7(3)**: 034010. https://doi.org/10.1088/1748-9326/7/3/034010

Gogoi, P.P., Vinoj, V., Swain, D., Roberts, G., Dash, J. and Tripathy, S., 2019. Land use and land cover change effect on surface temperature over Eastern India. *Scientific Reports,* **9(1)**: 1-10. https://doi.org/10.1038/s41598-019-45213-z

Li, Z.L., Tang, B.H., Wu, H., Ren, H., Yan, G., Wan, Z., … Sobrino, J.A., 2013. Satellite-derived land surface temperature: Current status and perspectives. *Remote Sensing of Environment,* **131**: 14-37. https://doi.org/10.1016/j.rse.2012.12.008

Longobardi, P., Montenegro, A., Beltrami, H. and Eby, M., 2016. Deforestation induced climate change: Effects of spatial scale. *PLoS ONE,* **11(4)**: https://doi.org/10.1371/journal.pone.0153357

Luintel, N., Ma, W., Ma, Y., Wang, B. and Subba, S., 2019. Spatial and temporal variation of daytime and nighttime MODIS land surface temperature across Nepal. *Atmospheric and Oceanic Science Letters,* **12(5)**: 305-312. https://doi.org/10.1080/16742834.2019.1625701

Marjuki, van der Schrier, G., Tank, A.M.G.K., van den Besselaar, E.J.M., Nurhayati and Swarinoto, Y.S., 2016. Observed trends and variability in climate indices relevant for crop yields in Southeast Asia. *Journal of Climate*, **29**(7): 2651-2669. https://doi.org/10.1175/JCLI-D-14-00574.1

Masson-Delmotte, V., Pörtner, H.-O., Skea, J., Zhai, P., Roberts, D. and Shukla, P.R., 2019. Global Warming of 1.5°C. Intergovernmental Panel on Climate Change.

Mboera, L.E.G., Mayala, B.K., Kweka, E.J. and Mazigo, H.D., 2011. Impact of climate change on human health and health systems in Tanzania: A review. *Tanzania Journal of Health Research*, **13**(5 SUPPL.ISS): 1-23. https://doi.org/10.4314/thrb.v13i1.10

Mishra, A.K., Singh, V.P. and Jain, S.K., 2010. Impact of global warming and climate change on social development. *Journal of Comparative Social Welfare*, **26**(2-3): 239-260. https://doi.org/10.1080/17486831003687626

Mitraka, Z. and Chrysoulakis, N., 2016. Earth observation for urban climate monitoring: surface cover and land surface temperature. *Intech*, i, 125-144. https://doi.org/http://dx.doi.org/10.5772/57353

Musyayyadah, H.A. and Vonnisa, M., 2019. Analisa Pola Temperatur Udara Permukaan di Sumatera Barat Tahun 1980-2017. *Jurnal Fisika Unand*, **8**(1): 91-97.

Neukom, R., Steiger, N., Gómez-Navarro, J.J., Wang, J. and Werner, J.P., 2019. No evidence for globally coherent warm and cold periods over the preindustrial Common Era. *Nature*, **571**(7766): 550-554. https://doi.org/10.1038/s41586-019-1401-2

ORNL DAAC, 2018. MODIS and VIIRS Land Products Global Subsetting and Visualization Tool. https://doi.org/10.3334/ornldaac/1379

Parveen, N. and Ghaffar, A., 2019. Spatial and Temporal Relationship between NDVI and Land Surface Temperature of Faisalabad city from 2000-2015. *European Online Journal of Natural and Social Sciences*, **8**(1): 55-64.

Phan, T.N., Kappas, M. and Tran, T.P., 2018. Land surface temperature variation due to changes in elevation in Northwest Vietnam. *Climate*, **6**(28): 1-19. https://doi.org/10.3390/cli6020028

Poor, E.E., Jati, V.I.M., Imron, M.A. and Kelly, M.J., 2019. The road to deforestation: Edge effects in an endemic ecosystem in Sumatra, Indonesia. *PLoS ONE*, **14**(7): 1-13. https://doi.org/10.1371/journal.pone.0217540

Prevedello, J.A., Winck, G.R., Weber, M.M., Nichols, E. and Sinervo, B., 2019. Impacts of forestation and deforestation on local temperature across the globe. *PLoS ONE*, **14**(3): 1-18. https://doi.org/10.1371/journal.pone.0213368

Rahmad, R., Nurman, A. and Pinem, K., 2019. Impact of NDVI Change to Spatial Distribution of Land Surface Temperature (A Study in Medan City, Indonesia). *1st International Conference on Social Sciences and Interdisciplinary Studies (ICSSIS 2018)*, **208**: 167-171. https://doi.org/10.2991/icssis-18.2019.33

Rasiah, R., Al-Amin, A.Q., Chowdhurry, A.H., Ahmed, F. and Zhang, C., 2018. Climate change mitigation projections for ASEAN. *Journal of the Asia Pacific Economy*, **23**(2): 195-212. https://doi.org/10.1080/13547860.2018.1442145

Rijal, S., Saleh, M.B., Surati, I.N. and Tiryana, T., 2016. Deforestation Profile of Regency Level in Sumatra. *International Journal of Sciences: Basic and Applied Research (IJSBAR)*, **25**(2): 385-402.

Saputra, M.H. and Lee, H.S., 2019. Prediction of Land Use and Land Cover Changes for North Sumatra, Indonesia, Using an Artificial-Neural-Network-Based Cellular Automaton. 1–16. https://doi.org/10.3390/su11113024

Stroppiana, D., Antoninetti, M. and Brivio, P.A., 2014. Seasonality of MODIS LST over Southern Italy and correlation with land cover, topography and solar radiation. *European Journal of Remote Sensing*, **47**(1): 133–152. https://doi.org/10.5721/EuJRS20144709

Sun, Q., Wu, Z. and Tan, J., 2012. The relationship between land surface temperature and land use/land cover in Guangzhou, China. *Environmental Earth Sciences*, **65**(6): 1687-1694. https://doi.org/10.1007/s12665-011-1145-2

Team, R.C., 2018. R: A Language and Environment for Statistical Computing. Retrieved February 2, 2019, from Vienna, Austria website: https://www.r-project.org/

Vadrevu, K., Heinimann, A., Gutman, G. and Justice, C., 2019. Remote sensing of land use/cover changes in South and Southeast Asian Countries. *International Journal of Digital Earth*, **12**(10): 1099-1102. https://doi.org/10.1080/17538947.2019.1654274

Wan, Z., Hook, S. and Hulley, G., 2015. MOD11A2 MODIS/Terra Land Surface Temperature and Emissivity 8-Day L3 Global 1km SIN Grid V006. *NASA EOSDIS Land Processes DAAC*. Retrieved from https://modis.ornl.gov/subsetdata/07Jan2019_11:57:25_7491008552L28.658558L77.1221S81L81_MOD11A2/citation.bib

Wan, Zhengming, 2008. New Refinements and Validation of the MODIS Land-Surface Temperature/Emissivity Products. *Remote Sensing of Environment*, **140**. https://doi.org/10.1016/j.rse.2006.06.026

Wongsai, N., Wongsai, S. and Huete, A.R., 2017. Annual seasonality extraction using the cubic spline function and decadal trend in temporal daytime MODIS LST data. *Remote Sensing*, **9**(12). https://doi.org/10.3390/rs9121254

Wu, X., Lu, Y., Zhou, S., Chen, L. and Xu, B., 2016. Impact of climate change on human infectious diseases: Empirical evidence and human adaptation. *Environment International*, **86**: 14-23. https://doi.org/10.1016/j.envint.2015.09.007

Yang, L., Qin, G., Zhao, N., Wang, C. and Song, G., 2012. Using a generalized additive model with autoregressive terms to study the effects of daily temperature on mortality. *BMC Medical Research Methodology*, **12**. https://doi.org/10.1186/1471-2288-12-165

Publication 2

INDONESIAN JOURNAL OF
GEOGRAPHY

RESEARCH ARTICLE

Land Surface Temperature Assessment in Central Sumatra, Indonesia

Tofan Agung Eka Prasetya [1,2 *], Munawar [1,3], Muhamad Rifki Taufik [4], Sarawuth Chesoh [1], Apiradee Lim [1], and Don McNeil[1]

[1] Research Methodology, Department of Mathematics and Computer Science, Faculty of Science and Technology, Prince of Songkla University, Pattani Campus, Thailand.

[2] Health Department, Faculty of Vocational Studies, Universitas Airlangga, Indonesia.

[3] Statistic Department, Faculty of Mathematics and Science, Syah Kuala University, Indonesia.

[4] Faculty of Health Science, University of Darussalam Gontor, Indonesia

Abstract Land Surface Temperature (LST) assessment can explain temperature variation, which may be influenced by factors such as elevation, land cover, and the normalized difference vegetation index (NDVI). In this study, a multiple linear regression model of LST variation was constructed based on data from the Moderate Resolution Imaging Spectroradiometer (MODIS) aboard NASA's Terra satellite, relating to the period, 2000-2018. The highest LST variation of nearly 1.3 °C/decade was found in savanna areas while the lowest variation was in the evergreen broadleaf forest and woody savanna, which experienced a decrease of 2.1 °C/decade. The overall mean change of LST was -0.4 °C/decade and the regression model with LST as the dependent variable and elevation, land cover type, and NVDI as independent variables produced an R square of 0.376. The variation in LST was different depending upon the NDVI.

Correspondent email:
sarawuth.c@psu.ac.th

1. Introduction

Climate change, particularly rising temperatures, is the most significant environmental problem facing the world today (Me-Ead & McNeil, 2016). Climate data based on satellite imaging of land surface temperature (LST) are essential in monitoring and assessing climate change impacts at both the small-and large-area scales (Wongsai et al. , 2017). Some critical factors in studying the temperature of the land surface are land cover, and whether the land is covered by green vegetation, as measured by the normalized difference vegetation index (NDVI), as well as elevation (Alavipanah et al., 2015; Guan et al., 2014; Q. Sun et al., 2012). Moreover, elevation has been a factor considered in previous studies that have modeled land cover (Palit & Popovic, 2005) since the change in elevation can contribute to differences in LST (Gao et al., 2008).

Deforestation has been estimated to have caused a 17 % increase in greenhouse gas emissions worldwide and is believed to be a factor in the increase in the earth's temperature (Gullison et al., 2007). A previous study of land-cover change on Sumatra showed that this island has the highest deforestation rate in Indonesia (Rijal et al., 2016). Between 1990 and 2010, 70 % of the forests on Sumatra were destroyed, with the highest rate of deforestation occurring in central Sumatra, including Riau Province, which suffered approximately 42 % deforestation (Goetz et al., 2012). Nevertheless, based on a previous study, the LST change in central Sumatra has been lower than in other regions of Sumatra (Prasetya et al., 2020). Previous studies have assessed the relationship between land cover and LST (Sobrino et al., 2013; Voogt & Oke, 2003; Zhou et al., 2011; Zhou et al.,

2014), the impact of different kinds of land cover on LST and how that relationship is affected by extreme land surface temperatures (Alavipanah et al., 2015; Vasishth, 2015; Zhou et al., 2014; Zhou et al., 2011). In a further study which explored the spatial variations in urban LST, the potential factors were grouped into categories by land use-land cover changes (LUCC) composition, biophysical conditions, the intensity of human activities, and landscape pattern (Weng et al., 2008). With the results showing that biophysical variables were significant in explaining the spatial variations in LST.

Another variable that can affect the LST is green vegetation cover, as measured by the NDVI. The NDVI is a tool for analyzing the vegetation status in the present and past and predicts its future condition (Onyia et al., 2018) and NDVI can be studied based on Moderate Resolution Imaging Spectro-radiometer (MODIS) observations which capture the spectral behavior of vegetation (Sharma et al., 2018). This is because plants react differently to different parts of the electromagnetic spectrum including visible light, and electromagnetic waves are typically absorbed in the red and blue wavelengths, so that reflected light retains the green wavelengths, with strong reflections also in the near-infrared (NIR) wavelengths (Sharma et al., 2018). Areas that have a high LST often have a low NDVI and vice versa (Chuai et al., 2013), and areas with a lower temperature are usually those with vegetation and bodies of water (Joshi & Bhatt, 2012). Yuan and Bauer (2007) found a negative correlation between NDVI and LST in a study of urban climate, and another study found that LST was correlated with NDVI and land use types, with a negative correlation between LST and certain

types of vegetation (Weng et al., 2004).

However, elevation, land cover, and NDVI might interact with each other. Although most previous studies have examined the effect of these factors separately. Thus, this study aimed to investigate the effects of the combination of elevation, land cover, and NDVI on changes in LST in central Sumatra.

2. The Methods

The study used data freely available from the MODIS aboard NASA's Terra satellite relating to LST, elevation, land cover, and NDVI (Kamel, 2015; Wan et al., 2015). The LST data were downloaded from the MODIS 8-day Terra LST (MOD11A2) from 2000 to 2018 at 0.05° spatial resolution. MODIS 8-day LST data are the mean of the data collected under clear-sky conditions only, and the elevation data were extracted from the LST data (ORNL DAAC, 2018; Phan et al., 2018; Wan, 2008). The land cover data and the NDVI data set (MOD13Q1) at a spatial resolution of 0.05° were also obtained from the MODIS MOD11A2 data set for the period 2000-2018.

The International Geosphere-Biosphere Program divides land cover into seventeen types (Friedl et al., 2005; Li et al., 2016). However, in this study, the land cover was simplified into nine categories, namely, evergreen broadleaf (EB) forest, woody (W) savanna, savanna, grassland, permanent (P) wetland, cropland, urban, cropland/natural vegetation

mosaic (Crop mos.), and water, by aggregating small areas that have similar characteristics. Elevation was categorized into nine groups: 0-14 meters above sea level (MASL); 15-29 MASL; 30-69 MASL; 70-149 MASL; 155-349 MASL; 350-599 MASL; 600-899 MASL; 600-899 MASL; 900-1199 MASL, and 1200+ MASL. For analysis, the NDVI was categorized into four categories that are A: below 0.75, B: 0.75 to 0.8 called constant, C: above 0.8 to 1 called changing, and above 0.75 combination between category B and C. Constant indicates that the trend in the NDVI was generally constant, changing indicates that the trend in NDVI was increasing during the study period and the fourth category was combining category B and C to reduce error in certain elevation category due to small size. The range of NDVI values is actually from -1 to 1, but an index range of 0.1 to 0.7 is typically indicative of vegetation. Thus healthy vegetation cover shows high index values while values near zero indicate bare soil and rock, where the near-infrared reflectance and the red levels are similar. Negative values indicate land cover types other than vegetation (e.g., water or snow) or clouds (Adeyeri & Okogbue, 2014). In this study, multiple linear regression was used to create a statistical model to investigate the effect of elevation, land cover, and NDVI with all analyses conducted using the R program (R Core Team, 2018).

Sumatra is one of the biggest islands in Indonesia (see Figure 1). The island was divided into 70 super regions with
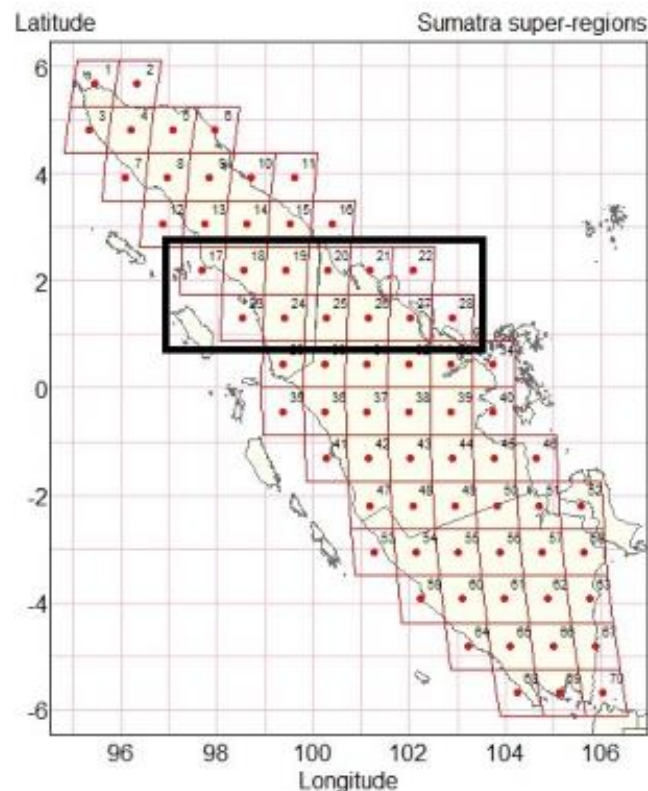

Figure 1. Sumatra Super regions and study area (bold box) in Central Sumatra

dimensions of 105 km × 105 km, and each super-region was divided into 25 regions with dimensions of 21 km × 21 km. Those regions were further subdivided into nine sub-regions with a dimension of 7 km × 7 km, each consisting of 1 km × 1 km squares represented by 49 pixels. In this study, six super-regions in the central part of Sumatra located in the equatorial area were chosen for analysis (super-regions 18, 19, 20, 24, 25, and 26). Other super regions in the area (super regions 17, 21, 22, 23, 27, and 28) were excluded because they consist largely of surface water (see Figure 1). In this study, MOD11A2 data for LST from MODIS covering Sumatra's equatorial area for the period 2000-2018 were collected from 1,274 sub-regions representing 61,300 pixels (Wan et al., 2015)

3. Result and Discussion

Table 1 shows the distribution by percentage of the land area studied in central Sumatra based on elevation, land cover, and NDVI. The largest area (14.9 %) is at an elevation of 30-69 MASL, with the area between 15-29 MASL having the lowest area (5 %). For the land cover, the highest and lowest areas are 48.3 % for EB Forest and 0.2 % for urban, respectively, while for NDVI, the category B accounts for the highest percentage (61.7 %), with the category C showing the lowest percentage (13.9 %).

Table 2 shows the increase in daily mean LST based on the four NDVI groups against elevation and land cover type,

and this is also illustrated in Figure 2. As can be seen, the highest increase in daily mean LST was recorded in savanna areas located above 600 MASL within the changing NDVI classification. The most considerable decrease in mean LST was recorded in the W. Savanna area located at 150-349 MASL within the NDVI < 0.75 classifications.

The data shown in Table 2, which were used to construct the multiple linear regression model, show that in central Sumatra, the mean land surface temperature had decreased by 0.4 °C/decade (horizontal red line in Figure 2). The highest increase in land surface temperature (1.29 °C/decade) occurred in savanna at an elevation above 600 MASL. Savanna, including woody-herbaceous systems and woody savanna, is generally defined as a subset of more widely distributed 'tree-grass' vegetation communities (Mildrexler et al., 2011), which constitute around 30 % of terrestrial vegetation (Grace et al., 2006). Trees contribute greater structural complexity to the savanna environment and aid the exchange of latent heat (Baldocchi et al., 2004). Baldocchi and Ma (2013) found, in a study conducted in America, that the air temperature potential in savanna areas is higher compared to other types of land cover, particularly grassland.

Figure 2 illustrates the data recorded in Table 2. According to Figure 2 (in areas of EB forest, which account for 48.3 % of the land-cover in central Sumatra), the NDVI is

Table 1. Elevation, NDVI and land cover in central Sumatra, 2000-2018

Variable	Frequency (pixels)	Percentage (%)
Elevation (meters above sea level)		
0-14	7,466	12.2
15-29	3,087	5.0
30-69	9,122	14.9
70-149	7,981	13.0
150-349	6,046	9.9
350-599	7,176	11.7
600-899	6,736	11.0
900-1199	6,847	11.2
1200+	6,839	11.1
Land-Cover		
EB Forest	29,581	48.3
W Savannas	21,992	35.9
Savannas	3,913	6.4
Grasslands	1,954	3.2
P Wetlands	291	0.5
Croplands	194	0.3
Urban	146	0.2
Crop.Mos	2,640	4.3
Water	589	0.9
NDVI pattern		
A: < 0.75	14,949	24.4
B: 0.75 - 0.8 constant	37,815	61.7
C: 0.8 – 1 changing	8,536	13.9

Table 2. Change in mean LST by NDVI, elevation and land cover in central Sumatra, 2000-2018

Variable	Change in mean LST per decade (°C)			
	NDVI < 0.75	NDVI 0.75- 0.8 constant	NDVI 0.8 - 1 changing	NDVI > 0.75 combined
E.B. Forest				
0-14 MASL	-0.69	-0.52	-0.44	NA
15-29 MASL	-0.40	-0.17	0.09	NA
30-69 MASL	-0.83	-0.21	0.27	NA
70-149 MASL	-1.61	-0.45	-0.00	NA
150-349 MASL	-2.09	-0.65	-0.64	NA
350-599 MASL	-1.23	-0.46	-0.39	NA
600-899 MASL	-0.77	-0.42	-0.33	NA
900-1199 MASL	-0.64	-0.33	-0.33	NA
1200+ MASL	-0.35	-0.01	0.90	NA
W. Savannas				
0-14 MASL	-0.49	-0.29	-0.11	NA
15-29 MASL	-0.15	0.04	0.20	NA
30-69 MASL	-0.48	0.23	0.58	NA
70-149 MASL	-1.19	-0.00	0.61	NA
150-349 MASL	**-2.11**	-0.64	-0.54	NA
350-599 MASL	-1.37	-0.59	-0.25	NA
600+ MASL	-0.59	-0.25	0.81	NA
Savannas				
0-599 MASL	-0.99	0.12	0.50	NA
600+ MASL	-0.60	0.47	**1.29**	NA
Grasslands	-0.35	0.60	1.24	NA
P. Wetlands	-0.95	-0.45	-0.09	NA
Croplands	-0.75	NA	NA	-0.44
Urban	-0.47	NA	NA	-0.45
Crop Mos.				
0-599 MASL	-1.56	NA	NA	-0.90
600+ MASL	-0.93	NA	NA	-0.54
Water	-1.25	NA	NA	-0.38

Note: NA indicates the absence of that land-cover type within a particular NDVI category, and NDVI > 0.75 combined category was combined between constant and changing due to small size.
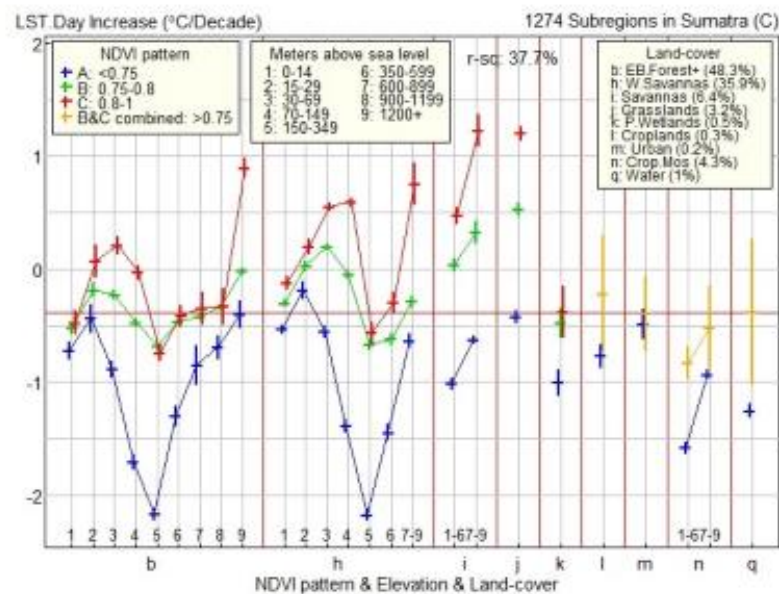

Figure 2. Change in daily LST (°C/decade) by NDVI, elevation and land cover of central Sumatra in 2000-2018

less than 0.75 and the elevation is lower than 600 MASL, and the LST has decreased by between 0.49 and over 2.1 °C/decade.

A previous study in Jaipur, India, showed that elevation has a negative correlation with LST (Baldocchi & Ma, 2013; Khandelwal et al., 2018) and research in China showed that in some areas the LST steadily decreases with increases in altitude, (Deng et al., 2018). Variation in temperature is thus often related to elevation, land cover and NDVI (Guha et al., 2018; Malbéteau et al., 2017)

Research on LUCC using remote sensing technology has a long history and has made considerable progress (Sun et al., 2012). LUCC is an essential indicator in understanding the interactions between human activities and the environment (Dewan et al., 2012). The linear change of temperature and its association with land cover depends on many environmental factors. For instance, urban land use is generally associated with high pollution, and temperature change (Sun et al., 2016) and urban environmental conditions often have a substantial impact on biodiversity, climate change, and atmospheric particulate pollution at local and global scales (Nagendra et al., 2004; Uy & Nakagoshi, 2007).

Forest cutting and deforestation have been found to cause significant increases in temperature of up to 0.28 (°C/decade on average in tropical regions (Li et al., 2016) and converting land use at high altitude from the forest or good quality vegetation will increase LST (Tang et al., 2018). Moreover, when the NDVI is low, the temperature is generally high

since the NDVI is negatively correlated with temperature (Dong et al., 2018).

However, in this study, the R square in the multiple regression constructed using the data shown in Table 2 was 0.376, which means that the elevation, land cover, and NDVI accounted for only 37.6 % of the change in the LST, indicating that 62.4 % of the variation was attributable to other factors. A previous study has suggested that while the NDVI is useful as a standard for estimating LST variation in urban areas, it may be less useful for other land cover classes, where there may be no correlation between LST and NDVI (Bakar et al., 2016).

As can be seen from Figure 3, where the initial NDVI was between 0 and around 0.75 (area A, accounting for 24.4 % of the land area), the mean decrease in LST per decade was 1.038 °C. On the other hand, where the initial NDVI was above 0.75 - 0.8 (area B, accounting for 61.7 % of the land area), the mean decrease in LST per decade was 0.27 °C, while for areas where the initial NDVI was above 0.8 (area C, accounting for 13.9 % of the land area), the mean increase in LST per decade was 0.268 °C. This finding shows that not all areas in central Sumatra experienced an increase in daily LST over the period studied. This study also confirms that in areas with healthy vegetation, the temperature did not significantly increase (Alipour et al., 2010; Deng et al., 2018).

Vegetation mapping and monitoring by satellite or remote sensing are essential to establish the vegetation conditions in a particular area. Vegetation monitoring by satellite imaging produces an inventory of green cover and
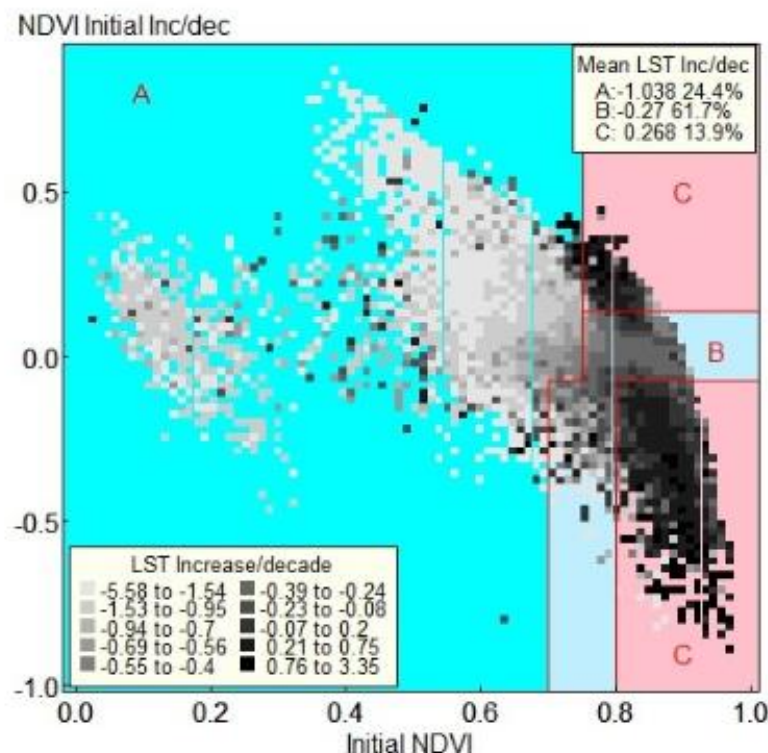

Figure 3. A plot of daily LST Increase (°C/decade) by initial NDVI

can be used for production forecasting, and vegetation growth assessment (Ozyavuz et al., 2015). Vegetation is a general term for plant life, which is the most abundant biotic element on Earth and reflects the extent of ground cover. The amount of vegetation is related to most of the factors which cause climate change, including temperature change.

4. Conclusion

This study concludes that variation in the LST in central Sumatra is related to change in land cover, NDVI, and elevation but that other factors are also implicated in the variation noted. This study demonstrates that LST change varies across different regions and that other factors need to be further investigated to establish the contribution of all variables to the LST. Even though the overall LST change in central Sumatra in Indonesia is within an acceptable range, with the average change in LST being only -0.4 °C/decade, the highest increase is 1.29 °C/decade and the most significant decrease is -2.11 °C/decade. Continuous monitoring of LST change is necessary for the broader area of Sumatra since deforestation, which is widespread throughout the island of Sumatra, maybe a significant contributory factor in LST change.

Acknowledgment

References

Adeyeri, O., & Okogbue, E. (2014). Effect of landuse landcover on surface temperature in Abuja using remote sensing and Geographic Information System (GIS). *Proceedings of Climate Change, and Sustainable Economic Development*, (November 2017), 175–184. https://doi.org/978-978- 521-43 -6-9

Alavipanah, S., Wegmann, M., Qureshi, S., Weng, Q., & Koellner, T. (2015). The role of vegetation in mitigating urban land surface temperatures: A case study of Munich, Germany during the warm season. *Sustainability*, 7(4), 4689–4706. https://doi.org/10.3390/su7044689

Alipour, T., Sarajian, M. ., & Esmaeily, A. (2010). Land surface temprature estimation from thermal band of landsat sensor, case study: Alashtar city. *The International Archives of the Photogrammetry, Remote Sensing and Spatial Information Sciences, XXXVIII*(2003), 1–6.

Bakar, S. B. A., Pradhan, B., Lay, U. S., & Abdullahi, S. (2016). Spatial assessment of land surface temperature and land use/land cover in Langkawi Island. *IOP Conference Series: Earth and Environmental Science*, 37(1). https://doi.org/10.1088/1755-1315/37/1/012064

Baldocchi, D. D., Xu, L., & Kiang, N. (2004). How plant functional-type, weather, seasonal drought, and soil physical properties alter water and energy fluxes of an oak-grass savanna and an annual grassland. *Agricultural and Forest Meteorology, 123*(1–2), 13–39. https://doi.org/10.1016/j.agrformet.2003.11.006

Baldocchi, D., & Ma, S. (2013). How will land use affect air temperature in the surface boundary layer? Lessons learned from a comparative study on the energy balance of an oak savanna and annual grassland in California, USA. *Tellus, Series B: Chemical and Physical Meteorology*, 65(1). https://doi.org/10.3402/tellusb.v65i0.19994

Chuai, X. W., Huang, X. J., Wang, W. J., & Bao, G. (2013). NDVI, temperature and precipitation changes and their relationships with different vegetation types during 1998-2007 in Inner Mongolia, China. *International Journal of Climatology*, 33(7), 1696–1706. https://doi.org/10.1002/joc.3543

Deng, Y., Wang, S., Bai, X., Tian, Y., Wu, L., Xiao, J., ... Qian, Q. (2018). Relationship among land surface temperature and LUCC, NDVI in typical karst area. *Scientific Reports*, 8(1), 1–12. https://doi.org/10.1038/s41598-017-19088-x

Dewan, A. M., Yamaguchi, Y., & Rahman, M. Z. (2012). Dynamics of land use/cover changes and the analysis of landscape fragmentation in Dhaka Metropolitan, Bangladesh. *GeoJournal*, 77(3), 315–330. https://doi.org/10.1007/s10708-010-9399-x

Dong, F., Chen, J., & Yang, F. (2018). A study of land surface temperature retrieval and thermal environment distribution based on landsat-8 in Jinan city. *IOP Conference Series: Earth and Environmental Science*, 108(4). https://doi.org/10.1088/1755-1315/108/4/042008

Friedl, M. A., Sulla-menashe, D., Tan, B., Schneider, A., Ramankutty, N., Sibley, A., & Huang, X. (2005). Remote sensing of environment MODIS collection 5 global land cover: Algorithm refinements and characterization of new datasets. *Remote Sensing of Environment*, 114(1), 168–182. https://doi.org/10.1016/j.rse.2009.08.016

Gao, M., Qin, Z., Qiu, J., Liu, S., Xu, B., Li, W., & Yang, X. (2008). Retrieving spatial-temporal variation of land surface temperature in Tibetan Plateau for the years 2005-2006 from MODIS satellite data. 7110 (June 2014), 71101A-71101A – 10. https://doi.org/10.1117/12.800098

Goetz, S., Hansen, M. C., Baccini, A., Tyukavina, A., Potapov, P., Margono, B. A., ... Turubanova, S. (2012). Mapping and monitoring deforestation and forest degradation in Sumatra (Indonesia) using landsat time series data sets from 1990 to 2010. *Environmental Research Letters*, 7(3), 034010. https://doi.org/10.1088/1748-9326/7/3/034010

Grace, J., José, J. S., Meir, P., Miranda, H. S., & Montes, R. A. (2006). Productivity and carbon fluxes of tropical savannas. *Journal of Biogeography*, 33(3), 387–400. https://doi.org/10.1111/j.1365-2699.2005.01448.x

Guan, Y., Dan, Q., Zhang, C., Cai, D., Liu, X., & Guo, S. (2014). Urban surface energy distribution and related characteristics: An remote sensing based research applied to the international livable cities. *Journal of Geo-Information Science*, 16(5), 806-814. https://doi.org/10.3724/SP.J.1047.2014.00806

Guha, S., Govil, H., Dey, A., & Gill, N. (2018). Analytical study of land surface temperature with NDVI and NDBI using Landsat 8 OLI and TIRS data in Florence and Naples city, Italy. *European Journal of Remote Sensing*, 51(1), 667–678. https://doi.org/10.1080/22797254.2018.1474494

Gullison, R. E., Frumhoff, P. C., Canadell, J. G., Field, C. B., Nepstad, D. C., Hayhoe, K., ... Nobre, C. (2007). Environment: tropical forests and climate policy. *Science*, 316(5827), 985–986.

Joshi, J. P., & Bhatt, B. (2012). Estimating temporal land surface temperature using remote sensing: A study of Vadodara urban area, Gujarat. *International Journal of Geology, Earth and Environmental Sciences*, 2(1), 123–130.

Kamel, D. (2015). MOD13Q1 MODIS/Terra Vegetation Indices 16-Day L3 Global 250m SIN Grid V006 [Data set]. https://doi.org/https://doi.org/10.5067/MODIS/MOD13Q1.006

Khandelwal, S., Goyal, R., Kaul, N., & Mathew, A. (2018). Assessment of land surface temperature variation due to change in elevation of area surrounding Jaipur, India. *Egyptian Journal of Remote Sensing and Space Science*, 21(1), 87–94. https://doi.org/10.1016/j.ejrs.2017.01.005

Li, Y., Zhao, M., Mildrexler, D. J., Motesharrei, S., Mu, Q., Kalnay, E., ... Wang, K. (2016). Potential and actual impacts of deforestation and afforestation on land surface temperature. *Journal of Geophysical Research*, 121(24), 14372–14386.

https://doi.org/10.1002/2016JD024969

Malbéteau, Y., Merlin, O., Gascoin, S., Gastellu, J. P., Mattar, C., Olivera-Guerra, L., ... Jarlan, L. (2017). Normalizing land surface temperature data for elevation and illumination effects in mountainous areas: A case study using ASTER data over a steep-sided valley in Morocco. *Remote Sensing of Environment*, 189, 25–39. https://doi.org/10.1016/j.rse.2016.11.010

Me-Ead, C., & McNeil, N. (2016). Graphical display and statistical modeling of temperature changes in tropical and subtropical zones. *Songklanakarin Journal of Science and Technology*, 38(6), 715–721.

Mildrexler, D. J., Zhao, M., & Running, S. W. (2011). A global comparison between station air temperatures and MODIS land surface temperatures reveals the cooling role of forests. *Journal of Geophysical Research: Biogeosciences*, 116(3), 1–15. https://doi.org/10.1029/2010JG001486

Nagendra, H., Munroe, D. K., & Southworth, J. (2004). From pattern to process: landscape fragmentation and the analysis of land use/land cover change. *Agriculture, Ecosystems & Environment*, 101(2), 111–115. https://doi.org/https://doi.org/10.1016/j.agee.2003.09.003

Onyia, N. N., Balzter, H., & Berrio, J. C. (2018). Normalized difference vegetation vigour index: A new remote sensing approach to biodiversity monitoring in oil polluted regions. *Remote Sensing*, 10(6), 1–34. https://doi.org/10.3390/rs10060897

ORNL DAAC. (2018). *MODIS and VIIRS Land Products Global Subsetting and Visualization Tool.* https://doi.org/10.3334/ornldaac/1379

Ozyavuz, M., Bilgili, B. C., & Salici, A. (2015). Determination of vegetation changes with NDVI method. *Journal of Environmental Protection and Ecology*, 16(1), 264–273.

Palit, A. K., & Popovic, D. (2005). *Computational Intelligence in Time Series Forecasting: Theory and Engineering Applications (Advances in Industrial Control).* Berlin, Heidelberg: Springer-Verlag.

Phan, T. N., Kappas, M., & Tran, T. P. (2018). Land surface temperature variation due to changes in elevation in northwest Vietnam. *Climate*, 6(28), 1–19. https://doi.org/10.3390/cli6020028

Prasetya, T. A. E., Munawar, Chesoh, S., Apiradee, L., & McNeil, D. (2020). Systematic measurement of temperature change in Sumatra Island☒: 2000-2019 MODIS data study. *Journal of Climate Change*, 6(1), 1–6. https://doi.org/10.3233/JCC200001

Rijal, S., Saleh, M. B., Surati, I. N., & Tiryana, T. (2016). Deforestation profile of regency level in Sumatra. *International Journal of Sciences: Basic and Applied Research (IJSBAR)*, 25(2), 385–402.

Sharma, I., Tongkumchum, P., & Ueranantasun, A. (2018). Modeling of land surface temperatures to determine temperature patterns and detect their association with altitude in the Kathmandu Valley of Nepal. *Chiang Mai University Journal of Natural Sciences*, 17(4), 275–288. https://doi.org/10.12982/CMUJNS.2018.0020

Sharma, I., Ueranantasun, A., & Tongkumchum, P. (2018). Modeling of satellite data to identify the seasonal patterns and trends of vegetation index in Kathmandu Valley, Nepal from 2000 to 2015. *Jurnal Teknologi*, 80(4), 125–133. https://doi.org/10.11113/jt.v80.11728

Sobrino, J. A., Oltra-carrió, R., Sòria, G., Jiménez-muñoz, J. C., Franch, B., Hidalgo, V., ... Paganini, M. (2013). Evaluation of the surface urban heat island effect in the city of Madrid. *International Journal of Remote Sensing*, 34(9), 3177–3192. https://doi.org/http://dx.doi.org/10.1080/01431161.2012.716548

Sun, L., Wei, J., Duan, D. H., Guo, Y. M., Yang, D. X., Jia, C., & Mi, X. T. (2016). Impact of land-use and land-cover change on urban air quality in representative cities of China. *Journal of Atmospheric and Solar-Terrestrial Physics*, 142(March 2019),

43–54. https://doi.org/10.1016/j.jastp.2016.02.022

Sun, Q., Wu, Z., & Tan, J. (2012). The relationship between land surface temperature and land use/land cover in Guangzhou, China. *Environmental Earth Sciences*, 65(6), 1687–1694. https://doi.org/10.1007/s12665-011-1145-2

Tang, B., Zhao, X., & Zhao, W. (2018). Local effects of forests on temperatures across Europe. *Remote Sensing*, 10(4), 1–24. https://doi.org/10.3390/rs10040529

R Core Team. (2018). R: A Language and Environment for Statistical Computing. Retrieved February 2, 2019, from Vienna, Austria website: https://www.r-project.org/

Uy, P. D., & Nakagoshi, N. (2007). Analyzing urban green space pattern and eco-network in Hanoi, Vietnam. *Landscape and Ecological Engineering*, 3(2), 143–157. https://doi.org/10.1007/s11355-007-0030-3

Vasishth, A. (2015). Ecologizing our cities: A particular, process-function view of southern California, from within complexity. *Sustainability (Switzerland)*, 7(9), 11756–11776. https://doi.org/10.3390/su70911756

Voogt, J. ., & Oke, T. . (2003). Thermal remote sensing of urban climates. *Remote Sensing of Environment*, 86(3), 370–384. https://doi.org/10.1016/S0034-4257(03)00079-8

Wan, Z. (2008). New refinements and validation of the MODIS land-surface temperature/emissivity products. In *Remote Sensing of Environment* (Vol. 140). https://doi.org/10.1016/j.rse.2006.06.026

Wan, Z., Hook, S., & Hulley, G. (2015). MOD11A2 MODIS/Terra Land Surface Temperature and Emissivity 8-Day L3 Global 1km SIN Grid V006. *NASA EOSDIS Land Processes DAAC*. Retrieved from https://modis.ornl.gov/subsetdata/07Jan2019_11:57:25_749108552L28.658558L77.1221S81L81_MOD11A2/citation.bib

Weng, Q., Liu, H., Liang, B., & Lu, D. (2008). The spatial variations of urban land surface temperatures: Pertinent factors, zoning effect, and seasonal variability. *IEEE Journal of Selected Topics in Applied Earth Observations and Remote Sensing*, 1(2), 154–166. https://doi.org/10.1109/JSTARS.2008.917869

Weng, Q., Lu, D., & Schubring, J. (2004). Estimation of land surface temperature–vegetation abundance relationship for urban heat island studies. *Remote Sensing of Environment*, 89(4), 467–483. https://doi.org/https://doi.org/10.1016/j.rse.2003.11.005

Wongsai, N., Wongsai, S., & Huete, A. R. (2017). Annual seasonality extraction using the cubic spline function and decadal trend in temporal daytime MODIS LST data. *Remote Sensing*, 9(12). https://doi.org/10.3390/rs9121254

Yuan, F., & Bauer, M. E. (2007). Comparison of impervious surface area and normalized difference vegetation index as indicators of surface urban heat island effects in Landsat imagery. *Remote Sensing of Environment*, 106(3), 375–386. https://doi.org/10.1016/j.rse.2006.09.003

Zhou, W., Huang, G., & Cadenasso, M. L. (2011). Does spatial configuration matter? Understanding the effects of land cover pattern on land surface temperature in urban landscapes. *Landscape and Urban Planning*, 102(1), 54–63. https://doi.org/10.1016/j.landurbplan.2011.03.009

Zhou, W., Qian, Y., Li, X., Li, W., & Han, L. (2014). Relationships between land cover and the surface urban heat island: Seasonal variability and effects of spatial and thematic resolution of land cover data on predicting land surface temperatures. *Landscape Ecology*, 29(1), 153–167. https://doi.org/10.1007/s10980-013-9950-5

Publication 3 (conference)

Different space characteristics of air temperature variation in North Sumatra Indonesia

T A E Prasetya[1,2 *], Munawar[1,3], S Chesoh[1], A Lim[1], and D R McNeil[1]

[1] Research Methodology, Departement of Mathematics and Computer Science, Faculty of Science and Technology, Prince of Songkla University, Pattani, Thailand
[2] Health Departement, Vocational Faculty, Universitas Airlangga, Surabaya, Indonesia
[3] Statistic Departement, Faculty of Mathematics and Science, Syah Kuala University, Aceh, Indonesia

*Email: tofan-agung-e-p@vokasi.unair.ac.id

Abstract. Land Surface Temperature (LST) can be used as an indicator of measuring temperature change in the regions. The changing variation can be produced or affected by some factors such as elevation, land cover products, and Normalized Difference Vegetation Index (NDVI). This study aimed to investigate LST variation based on elevation, land cover products, and NDVI in the North Sumatra area, Indonesia. Land products satellite data between 2000 and 2018 were downloaded from the moderate resolution imaging spectroradiometer (MODIS) website. Multiple linear regression was used to find the patterns of LST variation. The highest LST variation was found in Evergreen Broadleaf (EB) forest and urban area with the average change 0.4 and 0.5 °C/decade and the lowest was found in water surface area with the average change more than -1 °C/decade. The overall mean of LST changing was -0.1 °C/decade with r-square 31.4%. There was a unique LST variation in EB forest land cover when the elevation increased, the LST also increased from -0.4 to 0.5 °C/decade. The same condition also appears in Savannas and cropland/natural vegetation mosaic (Crop. Mos.). In conclusion, the changing of LST in North Sumatra was affected by elevation, land cover products, and NDVI.

1. Introduction

In recent years, climate change, particularly rising temperatures, is one of the important environmental problems facing the world today [1]. LST is the outer layer of temperature which is at the crossing point among superficial materials and the atmosphere [2]. LST is a satellite-based climate-related data that has an important part in controlling climatological processes, water stability at small to large-scale area and land surface energy interactions [3], [4].

The climate negatively affects human daylilies and environments [3]. This was represented in the long-term decreasing in the predominance of nutrition impairments, which slightly linked to extreme necessary events [5]. This was predominantly related to Southeast Asia since food production and security were at-risk sectors and Southeast Asia has a vital role as major exporter [6]. Since the 1950s, the tropics had become a source of enhancing interest among meteorologists because convective storms dominated the weather of the tropics. These develop mainly along the Intertropical Convergence Zone [1]. North Sumatra was one of the areas in Sumatra Island and it has tropic climate.

A study in Sumatra Island about land cover change (deforestation rate) shows that this island has the highest deforestation rate in Indonesia [7]. A study report that 70% of forests in Sumatra have been

destroyed since 1990 to 2010 [8]. Land degradation and deforestation in the North Sumatra area has been achieved 2.4 million hectares of land at risk [9]. Deforestation caused greenhouse gas emissions by 17% and believed as a factor of increasing the earth's temperature [10]. Thus, North Sumatra is selected to be a study area of whether the Land Surface Temperature (LST) was influenced by other factors namely land cover, NDVI, and elevation.

The elevation, land cover product, and normalized difference vegetation index (NDVI) were some potential determinants to analyze land surface temperature [11]–[13]. The high difference in land elevation has a significant effect on LST [14]. Remote sensing application in thermal detection has been applied in urban regions to estimate urban heat island, to threat land cover groups and as input for developing a model of urban surface-atmosphere exchange [15]. A study used correlation appraisals and multiple linear regressions to investigate the impacts of the structure and shape of land cover types on LST in Baltimore, Maryland, USA by considering Landsat Enhanced Thematic Mapper Plus (ETM+) image data [16]. It has been proposed that the effect directions of land cover variables on assessing LST were reliable throughout periods or seasons, although the significance of consequences, multifarious by periods or seasons, during summer were providing the strongest predictive ability and the weakest during winter [17].

Studies had been conducted to analyze the impact of the land cover on surface temperature and the effect of the extreme temperature in the land surface [18]. A study in the urban climate stated that NDVI and LST have no parallel value [19]. It means that in the high-temperature area has low NDVI and oppositely high NDVI is in the low-temperature area. Areas with high vegetation and water body have lower temperatures [20]. Some studies had been proposed to analyze the vegetation type and LST which had a negative correlation and associated with different land-use types [21], [22]. Therefore, this study considered elevation, land cover, and NDVI as an important factor to analyze LST in a tropical area, which is in North Sumatra. Moreover, this finding will confirm the existing phenomena occurring in the study region and favorable for the authority to set the environmental rehabilitation plans. Policymakers could use this study result to be focusing on a particular area of Sumatra that needs protection from increasing temperature and what caused it.

2. Materials and Methods

2.1. Study area
North Sumatra was selected as a study area. North Sumatra area was the northern part of Sumatra island and this land was between the Indian Ocean and the Strait Malacca. The border of on the northwest was Aceh and in the southeast, there were Riau and West Sumatra. This area stretches for at least 66.150 km² (refer to data-pixel). This area consists of the wetlands along the Strait of Malacca and Medan (the third-largest city in Indonesia) was located here. In the western and southern areas consisting of the plateau which was a stretch across the island of Sumatra. There is also Lake Toba, which located in the mountains, which was an ancient volcanic caldera. Most of the large islands around it on the west coast of the North Sumatra area were part of the North Sumatra province. We divided this area into super regions with a size of 11 regions in order to simplify the data obtained from the MODIS website. Only 6 super regions were selected for further analyses because from 10 super regions in the North Sumatra area, 4 of it has most areas connected to the sea (see Figure 1.)

2.2. Data source
LST, elevation, land cover, and NDVI data between 2000 and 2018 were downloaded from the moderate resolution imaging spectroradiometer (MODIS) website. LST data were extracted from MODIS 8-day Tera LST (MOD11A2) at 0.05° spatial resolution. These data are the average of the surface temperature clear sky condition, and elevation data was extracted from the United States geological survey (https://earthexplorer.usgs.gov/) data [23]–[25].

MODIS land cover dataset (MCD12C1) and MODIS NDVI dataset (MOD13Q1) provide land cover data annually from 2000-2018 at a spatial resolution of 0.05°. Land cover dataset contains 17 land cover

classes, namely evergreen needleleaf forest, evergreen broadleaf (EB) forest, deciduous needleleaf forest, deciduous broadleaf forest, mixed forest, closed shrublands, open shrublands, woody (W) savannas, savannas, grasslands, permanents wetlands, croplands, urban and built-up, cropland/natural vegetation mosaic (CropMos), snow and ice, barren or sparsely vegetated and water bodies. These were defined by the International Geosphere-Biosphere Programme classification [26], [27]. In this study, MODIS data from 1,125 sub-regions covered the North Sumatra area for the years 2000-2018 were collected. Land cover was simplified into 9 categories of land cover (evergreen broadleaf forest, woody savannas, savannas, grassland, permanents wetlands, croplands, urban, cropland/natural vegetation mosaic, and water) by aggregating the small percentage that has same characteristics.

Sumatra super regions contain 70 super regions. Each super-region consists of 25 regions with a size of 105 km × 105 km. Each region consists of 9 sub-regions with a size of 21 km × 21 km. Each sub-region has a size of 7 km × 7 km. Six super regions of the North Sumatra were chosen for statistical analysis which was super regions 8, 9, 10, 13, 14 and 15. Super regions 11 and 12 were not included in the analyses as most of the area is water (see Figure 1). 66.150-pixel data with 855 observations from 2000-2018 was used for this study for 6 super-region.

NDVI pattern grouped decide by using recursive partitioning decision tree and elevation also grouped for made the graph result readable. Elevation was categorized into 9 meters above sea level (MASL): 1. 0-14 MASL; 2. 15-29 MASL; 3. 30-69 MASL; 4. 70-149 MASL; 5. 155-349 MASL; 6. 350-599 MASL; 7. 600-899 MASL; 7. 600-899 MASL; 8. 900-1199 MASL; 9. 1200+ MASL. Land cover was simplified into 9 categories of land cover by aggregating the small percentage that has the same characteristics. The NDVI was categorized into 2 groups: 0.85 or more and less than 0.85. The range of Index values was from -1.0 to 1.0, but vegetation index values typically range between 0.1 and 0.7. Healthy vegetation cover has high index value and value near zero was an index for the area that reflects a similar level of near-infrared and red such as bare soil and rock. A negative value was for cloud, water, and snow which is the opposite of vegetation[28]. ARIMA coefficient was used in this study to take out the autocorrelation of LST-day data. All of the analysis, graph, and map was created by using the R program [29].
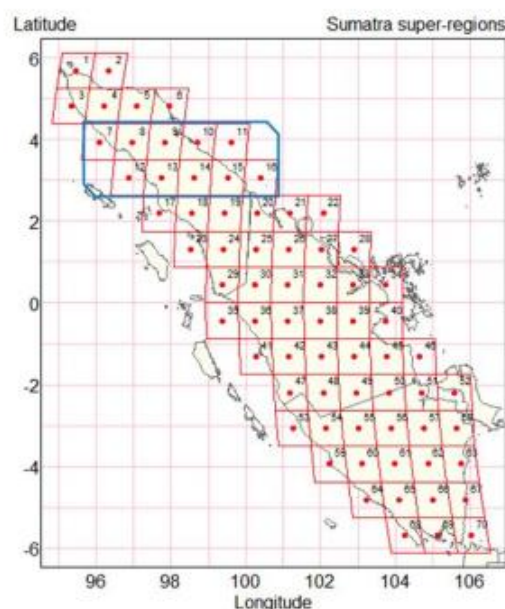

Figure 1. Super regions of Sumatra and North Sumatra with the center of latitude and longitude

3. Results and Discussion

This study consisted of 9 land cover products. The biggest area was the evergreen broadleaf forest (EB forest) accounted for 59.5% of land covers. The smallest area was water accounted for 1.2% of land covers (See figure 2). The other land cover areas with similar characteristics and small areas were aggregated into the same land cover area. The overall r-square was 31.4%. This means that elevation, land cover and NDVI influenced LST by 31.4%, and remained 68.6% affected by the other factors. Based on the result of this study, NDVI indicated vegetation for estimating LST in urban heat islands. But the results showed that land cover classes were not effective in some islands as we can see the correlation with LST [30]. The other study revealed that in highland areas, spatial heterogeneity in LST is also high due to surface landscape, land cover, superficial solar radiation, and more components [31].
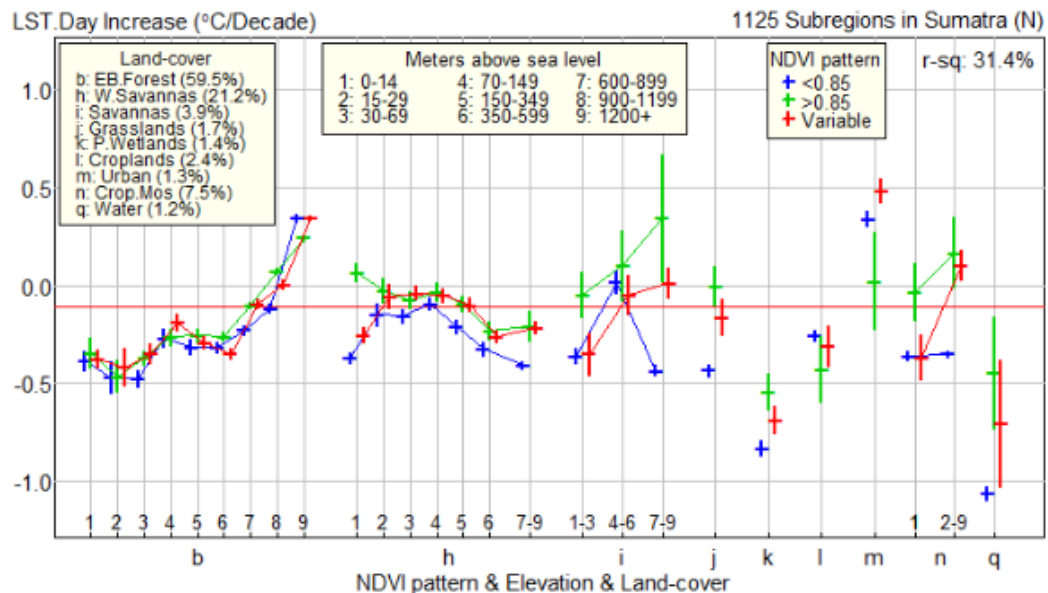

Figure 2. The LST day increase per decade (°C/decade) by NDVI, elevation and land cover of North Sumatra in 2000-2018

The highest increasing day LST was found in EB forest and in an urban area with 0.4 and 0.5 °C/decade. Both areas covered 59.5% and 1.3% of the North Sumatra area. The elevation of more than 1200 MASL with NDVI<0.85 happened in the EB forest. Changes in forest land cover conditions were a major factor in climate change in recent times [32]. Another study reported that land cover modification (deforestation) triggered major heating in the tropical area but forestation generated an opposing effect on the temperature change [26]. A study mentioned that on the local scale of the tropical area, deforestation and forestation obviously affected the changing of LST [33].

The water area covered 1.2% of land covers had the lowest LST day increase (°C/decade) approximately – 1 °C/decade. The water surface region was cooler in comparison with the other surface forms. A study in Turkey stated that the water area gives an effect on the land surface temperature around the water region[34]. The temperature changing also give significant influence in the environment (flora and fauna) and region topography related LST[35]. Due to water lets the light going profound into the deep flouting heat transmission during the day resulting in LST was in low value [36].

The LST variation of NDVI less than 0.85 was lower than the LST variation of NDVI at more than 0.85. It's mean that less vegetation in that area, the LST was decreasing at some level of elevation. The different condition was in urban and croplands, the LST change increased when NDVI less than 0.85. It's mean that less vegetation in that area, it had a higher temperature. A study in the urban developed

area in China had the highest LST [13]. The possible reason for decreased land surface temperature was because of the body water [37]. As we know that in the north Sumatra area there are Toba Lake that has a wide region water area.

Conclusions

Elevation, land cover changes and NDVI have related to LST Day Increase in the North Sumatra area that indicated the highest LST day increased was found in EB forest and urban area. Changing of elevation, land cover and NDVI contribute to the LST day increased. Although the overall characteristics of air temperature variation in north Sumatra of Indonesia are in the tolerable range, persistent monitoring is necessary.

Acknowledgments

Conflict of Interest

The authors declare no conflict of interest. This research is original research, there is no potential conflict of interest.

References

[1] A. W. Utomo, A. Suprayogi, and B. Sasmito, "Analisis hubungan variasi land surface temperature dengan kelas tutupan lahan menggunakan data citra satelit landsat (Studi Kasus : Kabupaten Pati)," *Jurnal Geodesi Undip*, vol. 2, no. April, pp. 13–22, 2013.

[2] D. Stroppiana, M. Antoninetti, and P. A. Brivio, "Seasonality of MODIS LST over Southern Italy and correlation with land cover, topography and solar radiation," *European Journal of Remote Sensing*, vol. 47, no. 1, pp. 133–152, 2014.

[3] N. Wongsai, S. Wongsai, and A. R. Huete, "Annual seasonality extraction using the cubic spline function and decadal trend in temporal daytime MODIS LST data," *Remote Sensing*, vol. 9, no. 12, 2017.

[4] Z. L. Li *et al.*, "Satellite-derived land surface temperature: Current status and perspectives," *Remote Sensing of Environment*, vol. 131, pp. 14–37, 2013.

[5] T. Wheeler and J. von Braun, *Climate Change Impacts on Global Food Security*, vol. 341. 2013.

[6] N. Alexandratos and J. Bruinsma, *World agriculture towards 2030/2050: the 2012 revision*, vol. 12–3. 2012.

[7] S. Rijal, M. B. Saleh, I. N. Surati, and T. Tiryana, "Deforestation Profile of Regency Level in Sumatra," *International Journal of Sciences: Basic and Applied Research (IJSBAR)*, vol. 25, no. 2, pp. 385–402, 2016.

[8] S. Goetz *et al.*, "Mapping and monitoring deforestation and forest degradation in Sumatra (Indonesia) using Landsat time series data sets from 1990 to 2010," *Environmental Research Letters*, vol. 7, no. 3, p. 34010, 2012.

[9] E. A. Perbatakusuma and F. Kaprawi, "Kajian spasial lahan kritis berbasis sistim informasi geografis untuk rehabilitasi kawasan koridor satwa liar dan harangan desa di kawasan hutan batang toru provinsi sumatera utara Program Ikon Koridor To Sigadis," 2011.

[10] R. E. Gullison *et al.*, "ENVIRONMENT: Tropical Forests and Climate Policy," *Science*, vol. 316, no. 5827, pp. 985–986, 2007.

[11] S. Alavipanah, M. Wegmann, S. Qureshi, Q. Weng, and T. Koellner, "The Role of Vegetation in Mitigating Urban Land Surface Temperatures: A Case Study of Munich, Germany during the Warm Season," *Sustainability*, vol. 7, no. 4, pp. 4689–4706, 2015.

[12] Y. Guan, Q. Dan, C. Zhang, D. Cai, L. I. U. Xuying, and 郭杉 GUO Shan, "Urban Surface Energy Distribution and Related Characteristics : An Remote Sensing Based Research Applied to the International Livable Cities," *Journal of Geo-Information Science*, vol. 16, no. 5, p. 806–814.,

2014.

[13] Q. Sun, Z. Wu, and J. Tan, "The relationship between land surface temperature and land use/land cover in Guangzhou, China," *Environmental Earth Sciences*, vol. 65, no. 6, pp. 1687–1694, 2012.

[14] M. Gao *et al.*, "Retrieving spatial-temporal variation of land surface temperature in Tibetan Plateau for the years 2005-2006 from MODIS satellite data," vol. 7110, no. June 2014, p. 71101A–71101A–10, 2008.

[15] J. . Voogt and T. . Oke, "Thermal remote sensing of urban climates," *Remote Sensing of Environment*, vol. 86, no. 3, pp. 370–384, Aug. 2003.

[16] W. Zhou, G. Huang, and M. L. Cadenasso, "Does spatial configuration matter? Understanding the effects of land cover pattern on land surface temperature in urban landscapes," *Landscape and Urban Planning*, vol. 102, no. 1, pp. 54–63, 2011.

[17] W. Zhou, Y. Qian, X. Li, W. Li, and L. Han, "Relationships between land cover and the surface urban heat island: Seasonal variability and effects of spatial and thematic resolution of land cover data on predicting land surface temperatures," *Landscape Ecology*, vol. 29, no. 1, pp. 153–167, 2014.

[18] A. Vasishth, "Ecologizing our cities: A particular, process-function view of southern California, from within complexity," *Sustainability (Switzerland)*, vol. 7, no. 9, pp. 11756–11776, 2015.

[19] F. Yuan and M. E. Bauer, "Comparison of impervious surface area and normalized difference vegetation index as indicators of surface urban heat island effects in Landsat imagery," *Remote Sensing of Environment*, vol. 106, no. 3, pp. 375–386, 2007.

[20] J. P. Joshi and B. Bhatt, "Estimating Temporal Land Surface Temperature Using Remote Sensing: a Study of Vadodara Urban Area, Gujarat," *International Journal of Geology, Earth and Environmental Sciences*, vol. 2, no. 1, pp. 123–130, 2012.

[21] Q. Weng, D. Lu, and J. Schubring, "Estimation of land surface temperature–vegetation abundance relationship for urban heat island studies," *Remote Sensing of Environment*, vol. 89, no. 4, pp. 467–483, 2004.

[22] W. Yue, J. Xu, and W. TAN, *The relationship between land surface temperature and NDVI with remote sensing: Application to Shanghai Landsat 7 ETM+ data*, vol. 28. 2007.

[23] ORNL DAAC, "MODIS and VIIRS Land Products Global Subsetting and Visualization Tool." ORNL Distributed Active Archive Center, 2018.

[24] T. N. Phan, M. Kappas, and T. P. Tran, "Land Surface Temperature Variation Due to Changes in Elevation in Northwest Vietnam," *Climate*, vol. 6, no. 28, pp. 1–19, 2018.

[25] Z. Wan, *New Refinements and Validation of the MODIS Land-Surface Temperature/Emissivity Products*, vol. 140. 2008.

[26] Y. Li *et al.*, "Potential and actual impacts of deforestation and afforestation on land surface temperature," *Journal of Geophysical Research*, vol. 121, no. 24, pp. 14372–14386, 2016.

[27] M. A. Friedl *et al.*, "Remote Sensing of Environment MODIS Collection 5 global land cover : Algorithm refinements and characterization of new datasets," *Remote Sensing of Environment*, vol. 114, no. 1, pp. 168–182, 2005.

[28] O. E. Adeyeri OE, "Effect of Landuse Landcover on Surface Temperature in Abuja Using Remote Sensing and Geographic Information System (Gis) ," *Proceedings of climate change, and sustainable economic development*, no. November, pp. 175–184, 2014.

[29] R. C. Team, "R: A Language and Environment for Statistical Computing," *Vienna, Austria*, 2018.

[30] S. B. A. Bakar, B. Pradhan, U. S. Lay, and S. Abdullahi, "Spatial assessment of land surface temperature and land use/land cover in Langkawi Island," *IOP Conference Series: Earth and Environmental Science*, vol. 37, no. 1, 2016.

[31] J. He, W. Zhao, A. Li, F. Wen, and D. Yu, "The impact of the terrain effect on land surface temperature variation based on Landsat-8 observations in mountainous areas," *International Journal of Remote Sensing*, vol. 40, no. 5–6, pp. 1808–1827, Mar. 2019.

[32] C. D. Allen, D. D. Breshears, and N. G. McDowell, "On underestimation of global vulnerability to

tree mortality and forest die-off from hotter drought in the Anthropocene," *Ecosphere*, vol. 6, no. 8, pp. 1–55, 2015.

[33] J. A. Prevedello, G. R. Winck, M. M. Weber, E. Nichols, and B. Sinervo, "Impacts of forestation and deforestation on local temperature across the globe," *PLoS ONE*, vol. 14, no. 3, pp. 1–18, 2019.

[34] Yıldız Demircioglu N., U. Advan, S. Yilmaz, A. Dagliyar, and A. Matzarakis, "Thermal Band Analysis of Agricultural Land Use and its Effects on Bioclimatic Comfort : The Case of Pasinler," *Proceedings of the Third International Conference on Countermeasures to Urban Heat Island*, vol. 16, no. DECEMBER, p. 15277, 2014.

[35] G. Jovanovska, U. Avdan, Z. Yigit Adan, and N. Demircioglu Yildiz, "Land Surface Temperature Change After Construction of the Kozjak Dam Based on Remote Sensing Data," 2016.

[36] W. Liu, J. Feddema, L. Hu, A. Zung, and N. Brunsell, "Seasonal and diurnal characteristics of land surface temperature and major explanatory factors in Harris County, Texas," *Sustainability (Switzerland)*, vol. 9, no. 12, 2017.

[37] S. Guha, H. Govil, A. Dey, and N. Gill, "Analytical study of land surface temperature with NDVI and NDBI using Landsat 8 OLI and TIRS data in Florence and Naples city, Italy," *European Journal of Remote Sensing*, vol. 51, no. 1, pp. 667–678, 2018.

Vitae

Name **:** Mr. Tofan Agung Eka Prasetya

Student ID **:** 6120330011

Educational Attainment:

Degree	Name of Institution	Year of Graduation
B.N (Nursing)	Jember University	2011
M.OHS (Occupational Health and Safety)	Airlangga University	2013

Scholarship Awards during Enrollment:

1. Thailand's Education Hub for ASEAN Countries (TEH-AC) scholarship. Prince of Songkla University. Thailand.
2. Research scholarship from Graduate School. Prince of Songkla University. Thailand.

International Conference:

1. International Conference on Health Applied Science 2019. Surabaya. Indonesia. Hosted by Faculty of Vocational. Universitas Airlangga
2. 1st Borobudur International Symposium on Applied Science and Engineering (BIS-ASE). Magelang. Indonesia. Hosted by Universitas Muhammadiyah Magelang.

Publication :

1. Prasetya. T. A. E., Munawar. Chesoh. S., Apiradee. L., & McNeil. D. (2020). Systematic Measurement of Temperature Change in Sumatra Island : 2000-2019 MODIS Data Study. Journal of Climate Change. 6(1). 1–6. https://doi.org/10.3233/JCC200001
2. Prasetya. T. A. E., Munawar. M., Taufik. M. R., Chesoh. S., Lim. A.. & McNeil. D. (2020). LST Assessment in Central Sumatra. Indonesia. Indonesian Journal of Geography. 52(2). 239–245. https://doi.org/https://doi.org/10.22146/ijg.51327

3. Prasetya. T. A. E., Mukhadiroh. L., Farapti. Chesoh. S., & Lim. A. (2020). Factors Contributing to Nurse Productivity in Public Hospitals in Surabaya. Indonesia. Hospital Topics. 98(4). 145–154. https://doi.org/10.1080/00185868.2020.1798317

4. Prasetya. T A E., Munawar. Chesoh. S., Lim. A., & McNeil. D. R. (2020). Different space characteristics of air temperature variation in North Sumatra Indonesia. Journal of Physics: Conference Series. 1517. 12008. https://doi.org/10.1088/1742-6596/1517/1/012008